BIOCHEMISTRY
including biophysical chemistry & molecular biology

Article

pubs.acs.org/biochemistry

Factor Defining the Effects of Glycine Betaine on the Thermodynamic Stability and Internal Dynamics of Horse Cytochrome *c*

Rishu Jain,[†] Deepak Sharma,[‡] Sandeep Kumar,[†] and Rajesh Kumar*[,†]

[†]School of Chemistry and Biochemistry, Thapar University, Patiala 147004, India

[‡]Council of Scientific and Industrial Research, Institute of Microbial Technology, Sector 39A, Chandigarh, India

Supporting Information

ABSTRACT: A compatible osmolyte such as glycine betaine (GB) and low concentrations of a denaturant constrain the internal dynamics of natively folded carbonmonoxycytochrome *c* (NCO) at pH 7.0. GB and subdenaturing concentrations of guanidine hydrochloride (GdnHCl) or urea have a cumulative effect on the constrained dynamics of NCO. At higher denaturant concentrations, large-scale unfolding fluctuations dominate the dynamics and inclusion of GB opposes the structural fluctuations that cause unfolding of the protein. These deductions are made from kinetic and thermodynamic parameters measured for the CO dissociation reaction of NCO at varying concentrations of denaturant in the absence and presence of 1.0 M GB. Intermolecular docking between horse ferrocytochrome *c* and a denaturant or GB reveals that the denaturant-mediated constrained dynamics of the protein is due to polyfunctional interactions between the denaturant and different groups of protein while the GB-mediated restricted dynamics of the protein arises from both the direct interactions of GB with different side chains of Lys or Arg residues of the protein and indirect interactions of GB with the protein surface. Thermodynamic analysis of the thermal and GdnHCl-induced unfolding curves of ferrocytochrome *c* measured in the absence and presence of 1.0 M GB at pH 7.0 indicates that GB increases the thermodynamic stability of ferrocytochrome *c* at neutral pH. Analysis of thermal and urea-induced unfolding curves of ferricytochrome *c* measured at different GdnHCl concentrations in the absence and presence of 0.5−1.0 M GB at pH 7.0 and 3.8 suggests that GB counteracts the destabilizing effect of the denaturant at pH 7.0 but exhibits an additive effect on the destabilizing effect of the denaturant at pH 3.8.

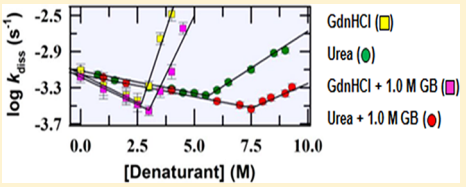

Proteins are multifarious systems that show extensive structural variability in their native state.[1] The native conformation of proteins under external stress such as dehydration, temperature variations, variable pH, freezing, high salinity, and internal stress such as high concentrations of denaturants can be stabilized by the accumulation of low-molecular weight organic molecules, termed as osmolytes or osmoprotectants.[2−7] Under protein stabilization conditions, many physicochemical approaches have provided significant evidence of the interaction of osmolytes with proteins.[8−18] However, because of the multifarious structures of the native proteins, an exact molecular explanation of the interaction of osmolytes with functional groups of proteins has not been reported. The osmolytes can interact with proteins both directly[19−22] and indirectly.[16,22−24] Few previous studies have suggested that the unfavorable interactions between the hydration surfaces of proteins and osmolytes stabilize the native conformation of proteins.[5,7,25−30]

The interrelationships among protein function, stability, and dynamics can play important roles in protein engineering and biological processes. Generally, the stability and dynamics of proteins in solution are strongly coupled to the dynamics of solvent.[31−35] Addition of osmolytes to the protein solution can alter the stability and internal dynamics of proteins.[7,12,20−23,25−27,30,36−39] Compatible osmolytes such as trimethylamine *N*-oxide (TMAO) and glycine betaine (GB) have been shown (i) to increase the thermodynamic stability of proteins,[2,3,5,8,17,29,30,40−42] (ii) to counteract the destabilizing effects of denaturants,[2,3,5,8,17,29,30,40−42] salts,[18,40] and hydrostatic pressure,[19,20,40] and (iii) to refold the partially denatured proteins.[9−12,40,43] Few earlier reports have also shown that compatible osmolytes such as TMAO and sucrose can restrict the internal dynamics of proteins.[36−38] The study presented here investigates the effect of a compatible osmolyte such as glycine betaine (GB) on the thermodynamic stability and internal dynamics of horse cytochrome *c* (cyt *c*). Being a single-domain fast folder protein, cyt *c* is widely used as a model for studying protein folding and dynamics.[44−48]

GB is an effective osmoprotectant and a compatible solute.[49−51] Earlier studies have revealed that the effect of GB on protein stability depends on the pH of the solution, the concentration of GB, and the types of proteins.[41,42] The study presented here shows that GB increases the thermodynamic stability of horse cyt *c* at neutral pH but decreases at mildly acidic pH. The major endeavor of this work is to demonstrate that GB counters the deleterious effect of denaturants (GdnHCl and urea) at neutral pH while it has cumulative effect on the deleterious effect of the denaturant at mildly acidic

Received: March 24, 2014
Revised: July 12, 2014
Published: July 31, 2014

   dx.doi.org/10.1021/bi500356c | *Biochemistry* 2014, 53, 5221−5235

pH values. While the counteraction effect of the osmolyte on the deleterious effect of denaturant (GdnHCl or urea) is studied extensively,[2,5,7,12−16,23,29] the additive effect of osmolytes on the denaturing effect of denaturants on proteins remained elusive.

Though fast protein motions that control conformational transitions responsible for biological functions have been extensively studied,[52,53] few studies that show relatively slow changes in the structural dynamics of proteins across the folding−unfolding transition are available.[54] By probing the changes in thermal fluctuations at the atomic and large-scale collective level, we can determine the possible roles of structural dynamics in folding. Although the effects of GdnHCl or urea on the structural fluctuation of native ferrocytochrome *c* (ferrocyt *c*) have been investigated,[55−57] the effect of GB on the structural fluctuation of natively folded carbonmonoxycytochrome *c* (NCO) has not been studied. Furthermore, the effect of GB on the structural fluctuation of NCO across the folding−unfolding transition of the protein remained elusive. This work determines the effect of GB on the structural fluctuation of NCO across the folding−unfolding transition by measuring the rate of thermally driven dissociation of CO from NCO at varying concentrations of the denaturant (GdnHCl or urea) in the absence and presence of 1.0 M GB at pH 7.0. Our results demonstrate that (i) GB and subdenaturing concentrations of urea and GdnHCl constrain the internal dynamics of NCO at neutral pH, (ii) GB and subdenaturing concentrations of the denaturant have a cumulative effect on the constrained dynamics of NCO, and (iii) from the subdenaturing to denaturing region, GB opposes the structural fluctuations that cause the structural unfolding of the protein. These results in conjugation with the results of docking between horse ferrocyt *c* and the denaturant (GdnHCl or urea) or GB show that the subdenaturing concentrations of the denaturant restrict the internal dynamics of the protein by establishing the polyfunctional interactions with different groups of the protein while the GB restricts the internal dynamics of the protein by making the direct interactions with different side chains of Lys or Arg residues of the protein or the N−H group of the peptide bond as well as indirect interactions with the protein surface.

MATERIALS AND METHODS

Horse heart cyt *c* (type VI, Sigma), GdnHCl (USB), urea (USB), and GB (Sigma) were used in all experiments without further purification. All experiments were conducted in either 50 mM sodium phosphate buffer (pH 7.0) or 25 mM sodium acetate buffer (pH 3.8). The required pH values of protein samples were adjusted by using concentrated HCl and NaOH solutions. The concentrations of GdnHCl and urea stock solutions were determined by refractive index measurements using Abbe's refractometer.[58]

Preparation of NCO and Measurement of CO Dissociation Kinetics. To prepare unfolded ferrocyt *c*, we initially dissolved ferricyt *c* in 6.5 M GdnHCl and then deaerated this unfolded protein solution by passing dry N_2 gas over it and reduced the solution by adding the freshly prepared sodium dithionite solution. The CO-liganded unfolded ferrocyt *c* (UCO) was prepared by passing dry CO gas over the unfolded ferrocyt *c* solution for ∼1 min under a dry N_2 gas atmosphere. NCO was prepared by adding ∼25 μL of the UCO solution to 2.0 mL of deaerated and dithionite-reduced refolding buffer containing the desired additive concentration. The final concentrations of protein and dithionite in reaction medium were ∼10.0 μM and 3.0 mM, respectively. The kinetics of CO dissociation were monitored on a Shimadzu UV−visible spectrophotometer at 550 nm heme absorbance, pH 7.0, and 25 °C. The dissociation of CO from NCO under denaturing conditions is relatively fast, so the kinetics of fast CO dissocition reactions were measured on a Shimadzu 2450 spectrophotometer coupled with an Applied Photophysics RX 2000 rapid kinetics stopped-flow mixing accessory.

Nuclear Magnetic Resonance (NMR) and CD Spectra of the NCO State of Cyt *c* in the Absence and Presence of Urea. Ferricyt *c* was unfolded in 10.0 M urea at pH 7.0. Unfolded ferricyt *c* thus obtained was deaerated under N_2 and was reduced by the addition of sodium dithionite. The reduced cyt *c* sample was allowed to bind CO under N_2 to form UCO. UCO was added to refolding buffer containing sodium dithionite and different concentrations of urea, at pH 7.0. The UCO was converted to NCO in refolding buffer. The NMR and CD spectra of the NCO state in the absence and presence of different concentratioins of urea were recorded on JEOL 400 MHz and Jasco 810 CD spectrophotometers, respectively. Deutarated urea was used for the NMR experiments.

GdnHCl-Induced Equilibrium Unfolding Measurements of Ferrocyt *c*. Samples of ferricyt *c* (∼5 μM) were prepared at different concentrations of GdnHCl ranging from 0 to 7.0 M at pH 7.0 in the absence and presence of 1.0 M GB. These ferricyt *c* samples were deaerated by being passed under N_2 gas and reduced by the addition of a freshly prepared sodium dithionite solution (∼3 mM) under continuous purging of dry N_2 gas. The ferrocyt *c* samples thus obtained were incubated for ∼0.5 h in tightly rubber capped glass test tubes at room temperature. Fluorescence (excitation at 280 nm) spectra of protein samples were recorded on Cary Eclipse Agilent spectrofluorometers at 25 °C.

Docking of Ferrocyt *c* with GB, GdnHCl, and Urea. To gain insight into the protein−denaturant (GdnHCl or urea) and protein−GB interactions, docking between horse ferrocyt *c* [Protein Data Bank (PDB) entry 2FRC][59] and the denaturant or GB was performed on the SwissDock server.[60,61] Briefly, the protein and denaturant or GB were uploaded in PDB and Mol2 formats, respectively, for docking on the SwissDock server. The HEME identifier was renamed from HEC to HEM because it was not detected by the SwissDock automated setup system as HEC. The structures of GB, urea, and $GdnH^+$ for docking were prepared by using ChemDraw and were converted to Mol2 files with the help of OpenBabel.[62] On submission of the docking assay, the CHARMM topology (parameters and coordinates) files were derived automatically from the Merck Molecular Force Field (MMFF).[63] Charges were also taken from MMFF.[64−68] The docking was executed by using the "Accurate" parameter at otherwise default parameters, with no region of interest defined (blind docking). Because our interest is to determine the putative different binding sites of GB, urea, and $GdnH^+$ with the entire target protein, therefore, the whole protein structure was considered during docking (blind docking). The different clusters of GB, urea, and $GdnH^+$ that were involved in binding with the protein at the same site were screened through their full fitness strength. Different binding modes of urea, $GdnH^+$, and GB−protein hydrogen bonding were analyzed using UCSF Chimera.[69]

Measurement of Thermal Unfolding of Ferrocyt *c*. To determine the effect of GB, GdnHCl, and urea on the thermal unfolding of ferrocyt *c*, we have collected the heme absorbance-

monitored (550 nm) and far-UV CD-monitored (222 nm, Jasco 810 CD spectrophotometer) thermal denaturation curves of ferrocyt *c* at varying concentrations of GB, GdnHCl, and urea at pH 7.0. The final concentrations of the protein and dithionite were ∼12 μM and ∼1.0 mM, respectively, for CD measurements and ∼10 μM and ∼3 mM, respectively, for absorbance measurements. For both CD and absorbance measurements, the Peltier-controlled heating rate was 1.0 °C/min.

Measurement of Thermal Unfolding of Ferricyt *c*. To investigate the effect of GB, GdnHCl, and urea on the thermal unfolding of ferricyt *c*, we have collected the far-UV CD-monitored (222 nm) thermal unfolding curves of ferricyt *c* at varying concentrations GB, GdnHCl, and urea at pH 7.0 and 3.8. The Peltier-controlled heating rate was 2.0 °C/min. The final protein concentration in the reaction medium was ∼10−12 μM.

Urea-Induced Equilibrium Unfolding Measurements of Ferricyt *c*. Samples of ferricyt *c* (∼5 μM) were prepared in 0−10.5 M urea for pH 7.0 and 0−8.0 M urea for pH 3.8 in the presence of different concentrations of GdnHCl in the absence and presence of 1.0 M GB. Protein samples thus obtained were incubated for 30 min at room temperature. Fluorescence spectra (excitation at 280 nm) of protein samples were recorded on a PerkinElmer LS-55 spectrofluorometer at 25 °C. The pH values of the samples are those measured after the experiment.

RESULTS

Thermal Dissociation of CO from NCO. The α-band (550 nm) in the electronic absorption spectrum of ferrocyt *c* at 20 °C and pH 7.0 is the main characteristic of the native Fe^{2+}−M80 bond of ferrocyt *c*.[70,71] The ligation of CO to Fe^{2+} of heme causes a decrease in the intensity or absorbance at 550 nm (Fe^{2+}−M80 + CO → Fe^{2+}−CO + M80) (Figure 1a). The dissociation of CO from the natively folded CO-liganded ferrocyt *c* (NCO) increases the intensity of the α-band (Fe^{2+}−CO + M80 → Fe^{2+}−M80 + CO) (Figure 1b). After ∼100-fold dilution of the UCO into CO-free refolding buffer, the UCO → NCO conversion precedes the NCO → N + CO (Fe^{2+}−CO + M80 → Fe^{2+}−M80 + CO) reaction. The concentration of CO decreases considerably in refolding buffer, and the intrinsic M80 ligand has an affinity for native ferrocyt *c* higher than that of CO; hence, the NCO → N + CO conversion results in the formation of the Fe^{2+}−M80 bond. The CO dissociation reaction described here is thermally driven and hence slow. Figure 1b shows a representative CO dissociation kinetic profile of NCO in the presence of ∼0.3 M GdnHCl (τ = 25 min), which indicates that the absorbance at 550 nm increases because of dissociation of the CO from NCO.

Nature of the CO Dissociation Reaction and GB Dependence of Log k_{diss}, $\Delta H_{diss}^{\ddagger}$, $\Delta S_{diss}^{\ddagger}$, and $\Delta\Delta S_{diss}^{\ddagger}$. Slow thermal dissociation of CO from NCO is basically a Fe^{2+}−CO + M80 → Fe^{2+}−M80 + CO displacement process,[72] in which the M80-resident part of protein serves as one reacting site.[73] It has been reported that cyt *c* forms an Ω-loop between residues 70 and 85[73] that exists in a partially unfolded form.[74,75] The collective motion of the M80-contaning Ω-loop of NCO is expected to regulate CO dissociation because (i) in its X-ray structure, the neighboring residues of M80 have considerably higher thermal factors and (ii) the local mobility of heme ring is suppressed by the intrinsic size and the rigidity of the ring system.[76] Figure 1c shows the variation of log k_{diss} as a function

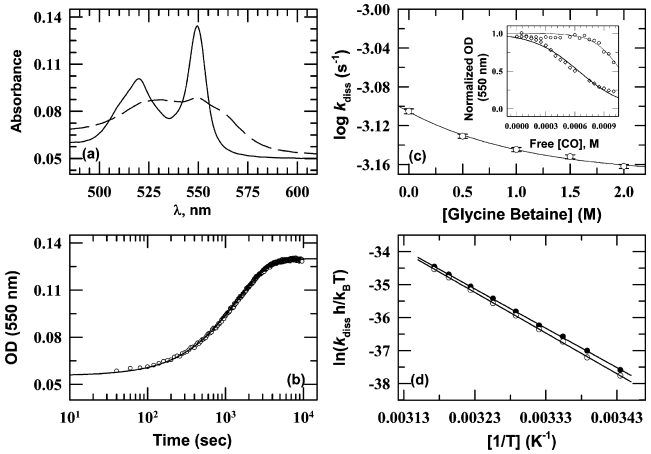

Figure 1. (a) Steady-state visible absorption spectra of NCO (−−−) and N (—) states at pH 7.0 and 25 °C. (b) Slow single-phase dissociation of CO from NCO, NCO → N + CO (τ = 25 min, 0.3 M GdnHCl, 25 °C). The NCO → N + CO reaction was probed at 550 nm, the λ_{max} of the N-state spectrum. The inset of panel c shows the CO titration of native ferrocyt *c* in the absence (◇) and presence of 1.0 M GB (○) at pH 7.0. Fits to data are according to the equation $y(x) = 1/[1 + 10^{n(x-K)}]$. (c) Effect of GB on rate of the CO dissociation reaction at 25 °C and pH 7.0. The line through data is drawn to guide the eye only and does not represent a functional dependence of k_{diss} on GB concentration. (d) Eyring plots for the CO dissociation reaction, in 50 mM phosphate buffer (pH 7.0), with no additives (●) and with 1.0 M GB (○).

of GB concentration. The variation of log k_{diss} with GB concentration demonstrates how the collective motions of the Ω-loop vary in response to GB in reaction milieu.

As the GB concentration is increased from 0.0 to 2.0 M, k_{diss} decreases by ∼1.5-fold. The decrease in log k_{diss} in the presence of GB provides a primary indication that GB decreases the level of structural fluctuation of the protein. The analysis of CO titrations of ferrocyt *c* (based on absorbance at 550 nm) collected in the absence and presence of 1.0 M GB at pH 7.0 (inset of Figure 1c) reveals that GB also decreases the affinity of CO for the active protein site (apparent dissociation constants, K_d, in the absence and presence of 1.0 M GB of ∼638.9 and ∼1078.4 μM, respectively). To further investigate the effect of GB on the structural fluctuation of the protein, we examined the GB dependence of the activation enthalpy ($\Delta H_{diss}^{\ddagger}$) and activation entropy ($\Delta S_{diss}^{\ddagger}$) of the CO dissociation reaction of NCO. The logic is that if the structural fluctuation of the protein is decreased at some concentration of GB, then the energy barrier or activation enthalpy for the CO dissociation reaction will be relatively higher. Figure 1d shows the Eyring plots for the CO dissociation reaction of NCO in the absence and presence of 1.0 M GB. To estimate the effect of GB on $\Delta H_{diss}^{\ddagger}$ and $\Delta S_{diss}^{\ddagger}$, the Eyring plots in Figure 1d were analyzed by using the Eyring equation[47,77]

$$\ln(k_{diss}h/k_BT) = \Delta S_{diss}^{\ddagger}/R - \Delta H_{diss}^{\ddagger}/RT \quad (1)$$

As expected, relative to the case in the absence of GB, the $\Delta H_{diss}^{\ddagger}$ value for the CO dissociation reaction increases in the presence of 1.0 M GB (ΔH_{diss} values of ∼24.4 and ∼25.3 kcal mol^{-1} in the absence and presence of 1.0 M GB, respectively). The conformational entropy loss for the CO dissociation reaction in the presence of GB relative to that in its absence ($\Delta\Delta S_{diss}^{\ddagger}$) was calculated according to eq 2

dx.doi.org/10.1021/bi500356c | *Biochemistry* 2014, 53, 5221−5235

$$\Delta\Delta S_{diss}^{\ddagger} = \Delta S_{diss}^{\ddagger}{}_{(x)} - \Delta S_{diss}^{\ddagger}{}_{(ref)} \quad (2)$$

where $\Delta S_{diss}^{\ddagger}{}_{(ref)}$ and $\Delta S_{diss}^{\ddagger}{}_{(x)}$ are the activation entropies for the CO dissociation reaction in the absence and presence of a GB concentration of x, respectively. Table 1 summarizes values

Table 1. Activation Enthalpies ($\Delta H_{ass}^{\ddagger}$), Activation Entropies ($\Delta S_{ass}^{\ddagger}$), and Conformational Entropy Losses ($\Delta\Delta S_{ass}^{\ddagger}$) for the Dissociation of CO from NCO at pH 7.0[a]

additive	[additive] (M)	$\Delta H_{diss}^{\ddagger}$	$\Delta S_{diss}^{\ddagger}$	$\Delta\Delta S_{diss}^{\ddagger}$
control	0.05	23.9 ± 0.2	6.8 ± 0.5	0.0
GB	1.0	24.7 ± 0.1	9.2 ± 0.5	2.4 ± 0.1
GdnHCl	2.5	27.9 ± 0.2	19.2 ± 0.6	12.4 ± 0.1
GdnHCl and 1 M GB	2.5	28.9 ± 0.4	21.9 ± 1.0	15.1 ± 0.5
GdnHCl	4.0	23.1 ± 0.3	7.0 ± 0.8	0.2 ± 0.3
GdnHCl and 1 M GB	4.0	24.0 ± 0.3	7.6 ± 0.8	0.8 ± 0.3
urea	5.5	27.8 ± 0.2	19.1 ± 0.5	12.3 ± 0.1
urea and 1 M GB	5.5	29.0 ± 0.3	22.5 ± 1.0	15.7 ± 0.5
urea	7.5	23.7 ± 0.3	6.6 ± 0.8	−0.2 ± 0.3
urea and 1 M GB	7.5	29.3 ± 0.2	23.0 ± 0.5	16.2 ± 0.1
urea	9.0	23.4 ± 0.1	6.5 ± 0.4	−0.2 ± 0.1
urea and 1 M GB	9.0	27.7 ± 0.4	18.6 ± 1.2	11.8 ± 0.7

[a] $\Delta H_{diss}^{\ddagger}$, $\Delta S_{diss}^{\ddagger}$, and $\Delta\Delta S_{diss}^{\ddagger}$ are reported in units of kilocalories per mole, calories per mole per kelvin, and calories per mole per kelvin, respectively. The uncertainty (standard error) is given.

of $\Delta\Delta S_{diss}^{\ddagger}$ in the absence and presence of 1.0 M GB. Clearly, $\Delta\Delta S_{diss}^{\ddagger}$ is apparently positive in the presence of GB (Table 1), which indicates that GB decreases the degree of motional freedom of the native protein at neutral pH.

Effect of GB on the ΔG_D and m_g of Ferrocyt *c*. Figure 2a shows the fluorescence-monitored normalized GdnHCl and urea denaturation curves of ferrocyt *c* in the absence and presence of 1.0 M GB at pH 7.0 and 25 °C. In the absence and presence of 1.0 M GB, ferrocyt *c* is completely unfolded in the presence of 6.0 M GdnHCl (Figure 2a), while within the limit of the aqueous solubilities of urea, ferrocyt *c* exhibits incomplete unfolding (Figure 2a).[47,77] Figure 2a also shows that the GdnHCl-induced unfolding curve of ferrocyt *c* shifts toward the higher concentration of GdnHCl in the presence of 1.0 M GB. Two-state analysis of the GdnHCl-induced unfolding curves of ferrocyt *c*[78] measured in the absence and presence of 1.0 M GB at 25 °C and pH 7.0 yields ΔG_D, the denaturation free energy, and m_g, which is proportional to the surface area exposed by the solvent. The values of ΔG_D and m_g are ∼17.1 kcal mol^{-1} and ∼3.3 kcal mol^{-1} M^{-1}, respectively, in the absence of GB, while the corresponding values in the presence of 1.0 M GB are 18.4 kcal mol^{-1} and 3.4 kcal mol^{-1} M^{-1}, respectively. This finding suggests that GB increases the thermodynamic stability of the protein.

Effect of GB on the Denaturant-Dependent Log k_{diss}. To test the effect of GB on the structural fluctuation of the native and denatured states of ferrocyt *c*, the rate coefficient of dissociation of CO from NCO was measured as a function of GdnHCl or urea concentration in the absence and presence of 1.0 M GB. Figure 2b shows the effect of GB on the denaturant (urea or GdnHCl) dependence of log k_{diss}. When the concentration of the denaturant in the reaction medium is increased from 0.0 to 5.0 M GdnHCl or 9.0 M urea, log k_{diss} initially decreases and then increases, displaying inflections

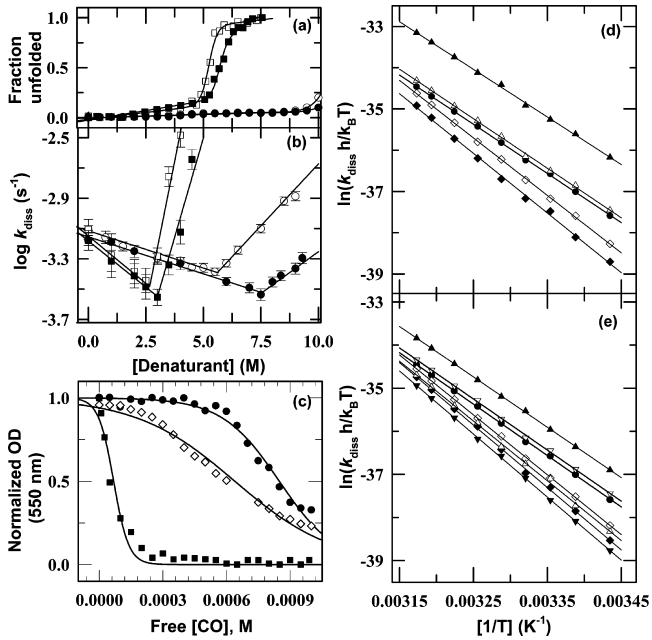

Figure 2. (a) Denaturant (GdnHCl and urea)-induced fluorescence-monitored normalized equilibrium unfolding curves of ferrocyt *c* measured in the absence [GdnHCl (□) or urea (○)] and presence of 1.0 M GB [GdnHCl (■) or urea (●)] at pH 7.0 and 25 °C. The solid curves are the fits of the data to a two-state equation.[78] The values of ΔG_D and m_g obtained are ∼17.1 kcal mol^{-1} and 3.3 kcal mol^{-1} M^{-1} and ∼18.4 kcal mol^{-1} and ∼3.2 kcal mol^{-1} M^{-1} for GdnHCl in the absence and presence of 1.0 M GB, respectively. (b) GdnHCl and urea dependence of log k_{diss} in the absence [GdnHCl (□) or urea (○)] and presence of 1.0 M GB [GdnHCl (■) or urea (●)] at pH 7.0 and 25 °C. (c) CO titration of native ferrocyt *c* in the absence (◇) and presence of 2.5 M GdnHCl (●) and 4.0 M GdnHCl (■) at pH 7.0. Fits to data are to the equation $y(x) = 1/[1 + 10^{n(x-K)}]$. (d) Eyring plots for the CO dissociation reaction, in 50 mM phosphate buffer (pH 7.0), with 0.05 M GdnHCl (●) or with 2.5 M GdnHCl in the absence (◇) and presence (◆) of 1.0 M GB or 4.0 M GdnHCl in the absence (▲) and presence (△) of 1.0 M GB. (e) Eyring plots for the CO dissociation reaction, in 50 mM phosphate buffer (pH 7.0), with 0.05 M GdnHCl (●) or with 5.5 M urea in the absence (◇) and presence (◆) of 1.0 M GB, 7.5 M urea in the absence (▽) and presence (▼) of 1.0 M GB, or 9.0 M urea in the absence (▲) and presence (△) of 1.0 M GB. Activation enthalpies, activation entropies, and conformational entropy losses relative to the native-state entropy are listed in Table 1.

centered at ∼2.5 M GdnHCl or ∼5.5 M urea in the absence of GB. The decrease in log k_{diss} in the subdenaturing limit of denaturants has been taken as evidence of the internal motional constraints of the protein in the subdenaturing limit of denaturant,[57] which tends to block the dissociation of CO from NCO. Recently, we have shown that in the subdenaturing limit, the polyfunctional interactions between protein groups and denaturants serve to cross-link different parts of the protein and thus restrict the internal dynamics of ferrocyt *c*.[77] ^{1}H NMR spectra can also be used to test the internal mobility and side chain environmental averaging of the protein in the presence of additives.[79,80] The NMR lines in the ^{1}H NMR spectrum of the NCO state (pH 7.0) are narrow and well-dispersed (Figure S1a of the Supporting Information). When 5.0 M urea is included, the spectrum appears to gain slightly more dispersion and sharpness of resonances all over the spectral width (Figure S1b of the Supporting Information). This finding indicates that in the presence of subdenaturing concentrations of the denatur-

dx.doi.org/10.1021/bi500356c | Biochemistry 2014, 53, 5221−5235

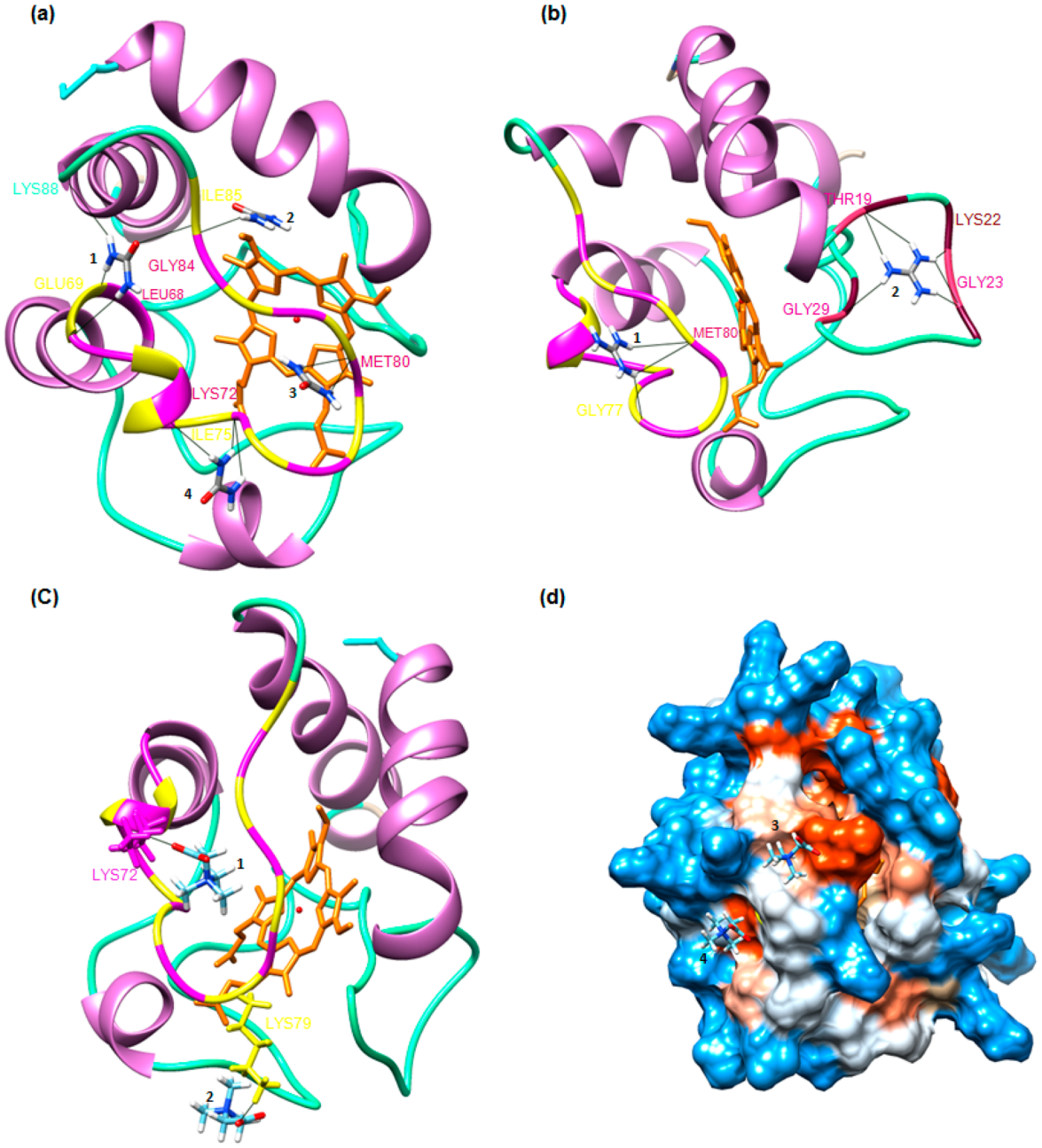

Figure 3. Representative result of docking between horse ferrocyt *c* (PDB entry 2FRC) and urea, $GdnH^+$, and GB. Panel a shows the hydrogen bonding network established by four urea molecules in which Lys72, Ile75, Met80, Gly84, and Ile85 residues of the Ω-loop are involved. Panel a clearly shows that these four urea molecules establish seven hydrogen bonds with different residues of the Ω-loop (Lys72, Ile75, Met80, Gly84, and Ile85) and three hydrogen bonds with other different residues of the protein (Leu68 and Glu69). Panel b represents the hydrogen bonding network established by two $GdnH^+$ ions. The first $GdnH^+$ ion (marked as 1) forms the two hydrogen bonds with different residues of the Ω-loop (Gly77 and Met80), while the other $GdnH^+$ ion (marked as 2) forms the six hydrogen bonds with different residues of the protein (Thr19, Lys22, Gly23, and Gly29). Panel c represents the direct single hydrogen bond established by each GB molecule (marked as 1 and 2) with the side chain of Lys72 or Lys79 of the Ω-loop. Panel d represents the two GB molecules (marked as 3 and 4) that do not form direct hydrogen bonds with the protein but are in contact with the protein surface via indirect interactions. Image processing was performed using UCSF Chimera.[69] The residues are marked according to their position.

ant, the internal protein interactions of the NCO state are slightly enhanced. At relatively higher denaturant concentrations (≥9.0 M urea), the NCO state becomes denatured as indicated by the loss of both chemical shift dispersion and line shape (Figure S1c of the Supporting Information). The far-UV CD spectra of the NCO state recorded in the absence and presence of 5.0 and 10.75 M urea also indicate that the high concentrations of the denaturant (≥9.0 M urea) denature the NCO state while the low concentrations of the denaturant stabilize the secondary structure of NCO (Figure S2 of the Supporting Information). The analysis of CO titrations of ferrocyt *c* measured in the absence and presence of 2.5 and 4.0 M GdnHCl at pH 7.0 (Figure 2c) further reveals that subdenaturing concentrations of the denaturant decrease the affinity of CO for the active protein site while the higher concentrations of the denaturant increase the affinity of CO for

dx.doi.org/10.1021/bi500356c | *Biochemistry* 2014, 53, 5221−5235

the active protein site (K_d values in the absence and presence of 2.5 and 4.0 M GdnHCl of ~638.9, 848.5, and 67.8 μM, respectively).

Both GB and subdenaturing concentrations of GdnHCl (<2.5 M) or urea (<5.5 M) individually decrease the rate of CO dissociation (Figures 1b and 2b); therefore, the coexistence of the two in reaction medium is expected to produce a cumulative effect on the rate of CO dissociation. The denaturant dependence of log k_{diss} in the absence and presence of 1.0 M GB is shown in Figure 2b. Figure 2b clearly shows that the rate−denaturant profile is shifted vertically down to a lower log k_{diss} in the presence of 1.0 M GB (Figure 2b). A horizontal shift toward a higher concentration of the denaturant is also apparent in the presence of 1.0 M GB (Figure 2b). Both vertical and horizontal shifts indicate that within the subdenaturing limit of the denaturant, GB shows a cumulative effect with the denaturant on the decrease in the level of structural fluctuation of the protein. In the subdenaturing to denaturing region, the increase in log k_{diss} (Figure 2b) can be interpreted to arise from protein destabilization and structural unfolding action of the denaturant[57] that would facilitate the dissociation of CO from NCO. Log k_{diss} increases to a lesser extent in the presence of 1.0 M GB than in its absence (Figure 2b), which indicates that the inclusion of GB opposes the structural fluctuation that causes the structural unfolding of the protein.

To investigate the effect of GB on the structural fluctuation of native and denatured states of ferrocyt *c* further, we have estimated the values of $\Delta H_{diss}^{\ddagger}$ and $\Delta S_{diss}^{\ddagger}$ for the CO dissociation reaction at different denaturant (GdnHCl or urea) concentrations in the absence and presence of 1.0 M GB. Figure 2d shows the Eyring plots for the CO dissociation reaction in the presence of 0.05 M GdnHCl without GB and in the presence of 2.5 and 4.0 M GdnHCl with and without 1.0 M GB. The Eyring plots for the CO dissociation reaction in the presence of 0.05 M GdnHCl without GB and in the presence of 5.0, 7.5, and 9.0 M urea with and without 1.0 M GB are shown in Figure 2e. The Eyring plots in panels d and e Figure 2 were analyzed by using the Eyring equation (eq 1).[47,77] The estimated values of $\Delta H_{diss}^{\ddagger}$ and $\Delta S_{diss}^{\ddagger}$ are summarized in Table 1. Clearly, in the presence of subdenaturing concentrations of denaturants, the denaturant-mediated increase in $\Delta H_{diss}^{\ddagger}$ is more pronounced in the presence of GB than in its absence, indicating that GB has a cumulative effect on the denaturant-mediated decreased structural fluctuations of the protein. On the other hand, in the subdenaturing to denaturing milieu, the denaturant-mediated decrease in $\Delta H_{diss}^{\ddagger}$ is less pronounced in the presence of GB than in its absence, indicating that GB counteracts the denaturant-mediated enhanced structural fluctuations of the protein.

The conformational entropy loss, $\Delta\Delta S_{diss}^{\ddagger}$, for the CO dissociation reaction in the presence of the denaturant relative to that in the absence of the denaturant in the absence and presence of 1.0 M GB was also calculated by using eq 2, and the values are summarized in Table 1. The data in Table 1 clearly show that within the subdenaturing limit of denaturants, the denaturant-mediated increase in $\Delta\Delta S_{diss}^{\ddagger}$ is more pronounced in the presence of GB than in its absence, suggesting that GB has a cumulative effect on the denaturant-mediated decreased degree of motional freedom of the protein.

***In Silico* Identification of GB, Urea, and GdnH$^+$ Binding Sites on Ferrocyt *c*.** The different clusters of GB, urea, and GdnH$^+$ that are involved in binding with the protein at the same site are screened through their full fitness strength. Docking results show that urea and GdnH$^+$ can form multiple variable length hydrogen bonds with the backbone−backbone or backbone−side chain atoms of the protein that are distant from each other, whereas the GB is not involved in cross-linking with different atoms of the protein that are distant from each other (Figure 3a−c and Table S1 of the Supporting Information). Docking results suggest that the 19 guanidinium ions can form 60 two hydrogen bonds (3.26 hydrogen bonds/GdnH$^+$) whereas the 28 urea molecules form 75 hydrogen bonds on different sites of the protein (2.67 hydrogen bonds/urea molecule). The docking results also reveal that the 12 GB molecules can form hydrogen bonds on different sites of the protein and the 14 GB molecules are in contact with protein surface via indirect interactions (polar or hydrophobic) (Figure 3d and Tables S1 and S2 of the Supporting Information). The representative results in Figure 3a clearly indicate that four urea molecules establish the seven variable length hydrogen bonds with different residues of the Ω-loop and the three variable length hydrogen bonds with other different residues of protein. Figure 3b clearly shows that one guanidinium ion can establish two variable length hydrogen bonds with different residues of the Ω-loop of the protein and another guanidinium ion forms the six variable length hydrogen bonds with different residues of the protein. Figure 3c shows that each GB molecule establishes a direct single hydrogen bond to side chains of the Lys residue. Figure 3d indicates that two GB molecules are in contact with the protein surface via indirect interactions (polar or hydrophobic).

Effect of GB on the Secondary Structures of Native and Denatured States of Ferricyt *c* at Neutral pH 7.0 and Mildly Acidic pH 3.8. The far-UV CD spectrum of ferricyt *c* at 25 °C exhibits a negative Cotton effect at 222 nm that reflects the secondary structure of the native protein at pH 7.0 (Figure 4a) or pH 3.8 (Figure 4b). When the temperature is

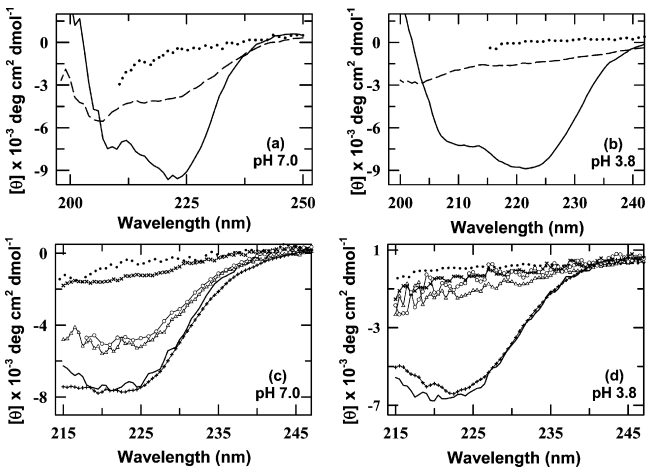

Figure 4. Effect of GB on native and denatured states of ferricyt *c*. Panels a and b present far-UV CD spectra of native (—, 25 °C) and temperature-denatured (−−−, 90 °C) and GdnHCl-denatured (···, 5.0 M GdnHCl) states of ferricyt *c* collected at pH 7.0 (a) and 3.8 (b). The far-UV CD spectra of native ferricyt *c* in the absence (−−−) and presence of 1.0 M GB (+) are shown in panels c and d at pH 7.0 and 3.8, respectively. Panels c and d also show the far-UV CD spectra of the denaturant-induced denatured state of ferricyt *c* (8.5 M urea and 5.0 M GdnHCl) in the absence [urea (×) and GdnHCl (●)] and presence of 1.0 M GB [urea (△) and GdnHCl (○)] at pH 7.0 and 3.8, respectively.

dx.doi.org/10.1021/bi500356c | *Biochemistry* 2014, 53, 5221−5235

increased from 25 to 90 °C or the denaturant concentration from 0.0 to 5.0 M GdnHCl, the negative Cotton effect is eliminated at pH 7.0 (Figure 4a) or pH 3.8 (Figure 4b), indicating that the secondary structure of the protein is significantly disrupted. Panels c and d of Figure 4 show the effect of GB on the far-UV CD spectra of native and denatured (by ∼5.0 M GdnHCl or ∼8.5 M urea) states of ferricyt *c* at pH 7.0 and 3.8, respectively, which reveals that the far-UV CD signals of native ferricyt *c* do not change significantly in the presence of 1.0 M GB, indicating that the GB does not greatly affect the secondary structure of the native protein (Figure 4c,d). However, in the presence of 1.0 M GB, the denatured protein gains some far-UV CD signals at pH 7.0, indicating that the GB induces the formation of the secondary structure of the denatured protein at pH 7.0 (Figure 4c).

Effect of GB on the T_m, ΔH_m, and ΔG_T of Cyt c in an Aqueous Solution. Panels a and b of Figure 5 show that in the presence of 1.0 M GB, the thermal unfolding curve of ferrocyt *c* is shifted to higher temperatures at pH 7.0. Panels c and d reveal that in the presence of 1.0 M GB, the thermal unfolding curve of ferricyt *c* is shifted to higher temperatures at pH 7.0 and shifted to lower temperatures at pH 3.8. The thermal unfolding curves were analyzed for the thermal denaturation midpoint (T_m), the enthalpy of denaturation (ΔH_m), and the heat capacity change (ΔC_p) by using a nonlinear least-squares method according to the Gibbs–Helmholtz equation

$$A(T) \text{ or } \theta(T) = \left[C_{pre} + m_{pre}T + (C_{post} + m_{post}T) \exp\left(\left\{\Delta H_m\left(\frac{T}{T_m} - 1\right) + \Delta C_p[T_m - T + T\ln(T/T_m)]\right\}/(RT)\right)\right]/\left[1 + \exp\left(\left\{\Delta H_m\left(\frac{T}{T_m} - 1\right) + \Delta C_p [T_m - T + T\ln(T/T_m)]\right\}/(RT)\right)\right] \quad (3)$$

where $A(T)$ or $\theta(T)$ is the observed variable parameter, c_{pre} and c_{post} represent intercepts of the native (pretransition) and unfolded (post-transition) baselines, respectively, and m_{pre} and m_{post} represent slopes of the native (pretransition) and unfolded (post-transition) baselines, respectively. For ferrocyt *c* and ferricyt *c*, the resulting T_m, ΔH_m, and ΔC_p values in the absence and presence of GB are listed in Table S3 of the Supporting Information and Table 2, respectively. In the presence of GB, T_m increases at pH 7.0 and decreases at pH 3.8 (Table S3 of the Supporting Information and Table 2). By using ΔH_m, T_m, and ΔC_p values and eq 4, the ΔG_T at 25 °C was determined as a function of GB concentration

$$\Delta G_T = \Delta H_m\left(1 - \frac{T}{T_m}\right) + \Delta C_p[T - T_m - T\ln(T/T_m)] \quad (4)$$

At pH 7.0, ΔG_T increases linearly with GB concentration, and hence, the *m* value that is equal to the slope of the ΔG_T versus GB concentration plot is positive (approximately 0.56) (inset of Figure 5c). However, at pH 3.8, ΔG_T decreases linearly and gives a negative *m* value (approximately −1.26) (inset of Figure 5d). These findings indicate that GB increases the thermodynamic stability of the protein at neutral pH and decreases it at mildly acidic pH.

Effect of GB on the Denaturant-Dependent T_m, ΔH_m, and ΔG_T Values of Cyt *c*. Figure 6a shows the representative heme absorption-monitored (550 nm) normalized denaturant (GdnHCl and urea)-dependent thermal unfolding curves of

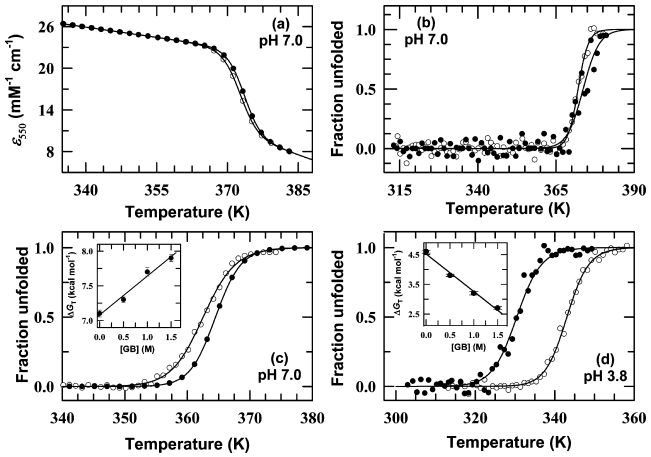

Figure 5. (a) Thermally induced unfolding of ferrocyt *c* monitored at 550 nm in the Soret region as the change in the excitation coefficient in the absence (○) and presence (●) of 1.0 M GB at pH 7.0. (b) Thermally induced unfolding of ferrocyt *c* monitored by CD at 222 nm in the absence (○) and presence (●) of 1.0 M GB at pH 7.0. (c and d) Far-UV CD-monitored thermal unfolding curves of ferricyt *c* measured at pH 7.0 and 3.8, respectively, in the absence (○) and presence (●) of ∼1.0 M GB. The solid curves in panels a–d represent nonlinear least-squares fits to the Gibbs–Helmholtz equation (eq 3). The insets of panels c and d show the variation of the change in thermal unfolding free energy, ΔG_T, of ferricyt *c* with GB concentration at pH 7.0 and 3.8, respectively. The solid lines in the insets of panels c and d represent linear least-squares fits of the ΔG_T vs [GB] data.

Table 2. GB Dependence of T_m, ΔH_m, ΔC_p, and ΔG_T Values for Thermal Unfolding of Ferricyt *c* (CD at 222 nm) at pH 7.0 and 3.8[a]

	pH 7.0				pH 3.8			
[GB] (M)	T_m (K)	ΔH_m (kcal mol^{-1})	ΔC_p (kcal mol^{-1} K^{-1})	ΔG_T (kcal mol^{-1})	T_m (K)	ΔH_m (kcal mol^{-1})	ΔC_p (kcal mol^{-1} K^{-1})	ΔG_T (kcal mol^{-1})
0.0	362.9	83.5	1.3	6.9	342.8	65.7	1.1	5.2
0.5	363.4	85.0	1.2	7.8	336.6	60.1	1.1	4.4
1.0	364.5	86.0	1.3	7.3	330.9	54.7	1.1	3.6
1.5	365.5	87.0	1.2	8.1	325.5	45.2	1.0	2.6

[a]The uncertainties of T_m, ΔH_m, ΔG_T, and ΔC_p values reported here are ±0.5 °C, ±2.0 kcal mol^{-1}, ±0.5 kcal mol^{-1}, and ±0.2 kcal mol^{-1} K^{-1}, respectively.

dx.doi.org/10.1021/bi500356c | *Biochemistry* 2014, 53, 5221–5235

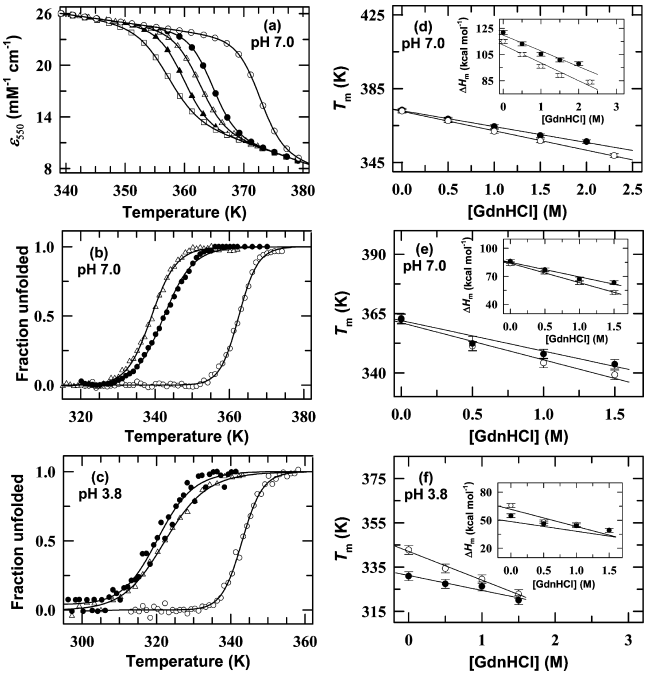

Figure 6. (a) Thermally induced unfolding of ferrocyt *c* monitored at 550 nm in the Soret region as the change in the excitation coefficient at pH 7.0, in the absence of a denaturant (○), in the presence of 3.0 urea (△), in the presence of 3.0 M urea with 1.0 M GB (●), in the presence of 1.5 M GdnHCl (□), and in the presence of 1.5 M GdnHCl with 1.0 M GB (▲). (b and c) Far-UV CD-monitored (222 nm) thermal unfolding curves of ferricyt *c* at pH 7.0 and 3.8, respectively, in the absence of an additive (○), in the presence of 1.5 M GdnHCl (△), and in the presence 1.5 M GdnHCl with 1.0 M GB (●). The solid curves in panels a–d represent nonlinear least-squares fits of the data to eq 3. (d) Variation of the thermal unfolding midpoint, T_m, of ferrocyt *c* as a function of GdnHCl concentration, in the absence (○) and presence (●) of 1.0 M GB at pH 7.0. The inset of panel d shows the variation of ΔH_m of ferrocyt *c* at pH 7.0 as a function of GdnHCl concentration in the absence (○) and presence (●) of 1.0 M GB. (e and f) Variation of T_m of ferricyt *c* at pH 7.0 and 3.8, respectively, as a function of GdnHCl concentration in the absence (○) and presence (●) of 1.0 M GB. Insets of panels e and f show the variation of ΔH_m of ferricyt *c* at pH 7.0 and 3.8, respectively, as a function of GdnHCl concentration in the absence (○) and presence (●) of 1.0 M GB. The solid lines in panels d–f and in the insets of panels d–f represent linear least-squares fits of the data.

ferrocyt *c* in the absence and presence of 1.0 M GB at pH 7.0. The representative far-UV CD-monitored (222 nm) GdnHCl-dependent normalized thermal unfolding curves of ferricyt *c* in the absence and presence of 1.0 M GB at pH 7.0 and 3.8 are shown in panels b and c of Figure 6, respectively. At pH 7.0 and 3.8, the thermal unfolding curve shifts to lower temperatures in the presence of a denaturant (Figure 6a–c). However, in the presence of 1.0 M GB, the denaturant-induced shift in the thermal unfolding curve is less pronounced at pH 7.0 (Figure 6a,b) and more pronounced at pH 3.8 (Figure 6c). To determine the effect of GB on the denaturant dependence of ΔH_m, T_m, and ΔC_p, the thermal unfolding curves of ferrocyt *c* and ferricyt *c* collected at various concentrations of GdnHCl or urea in the absence and presence of 1.0 M GB were analyzed using eq 3. The resulting T_m, ΔH_m, and ΔC_p are provided in Tables S4 and S5 of the Supporting Information. At pH 7.0 and 3.8, in the absence and presence of 1.0 M GB, T_m and ΔH_m were found to decrease linearly with GdnHCl concentration (Figure 6d–f). However, in the presence of 1.0 M GB, the decreases in T_m and ΔH_m with GdnHCl concentration are less pronounced at pH 7.0 (Figure 6d,e) and more pronounced at pH 3.8 (Figure 6f). The dependence of ΔH_m on T_m obtained by thermal unfolding of proteins in the presence of various concentrations of GdnHCl in the absence and presence of 1.0 M GB at pH 7.0 (Figure 7a,b) and pH 3.8 (Figure 7c) is shown

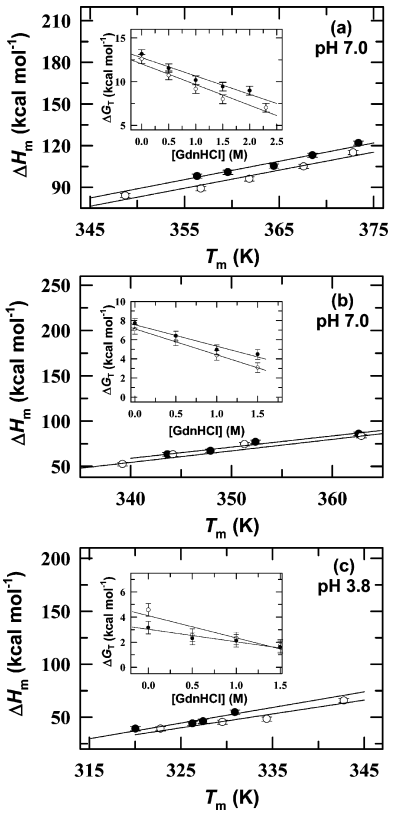

Figure 7. (a) Variation of ΔH_m as a function of the T_m of ferrocyt *c* (heme absorbance at 550 nm) at pH 7.0 obtained at different GdnHCl concentrations in the absence (○) and presence (●) of 1.0 M GB. The inset of panel b shows the variation of the ΔG_T of ferrocyt *c* as a function of GdnHCl concentrations at pH 7.0 in the absence (○) and presence (●) of 1.0 M GB. (b and c) Variation of ΔH_m as a function of the T_m of ferricyt *c* (CD at 222 nm) at pH 7.0 and 3.8, respectively, obtained at different GdnHCl concentrations in the absence (○) and presence (●) of 1.0 M GB. The insets in panels b and c show the variation of ΔG_T of ferricyt *c* as a function of GdnHCl concentration at pH 7.0 and 3.8, respectively, in the absence (○) and presence (●) of 1.0 M GB.

in Figure 7a–c. From the plots of ΔH_m versus T_m, ΔC_p values in the absence and presence of 1.0 M GB were determined by a linear least-squares fit of the data to eq 5[72−74]

$$\Delta H_m = \Delta C_p T_m + b \quad (5)$$

By using eq 4 and ΔC_p values (obtained by eq 5), the ΔG_T values were determined at 25 °C as a function of GdnHCl concentration in the absence and presence of 1.0 M GB. A number of previous studies of urea and GdnHCl denaturation of proteins have revealed that ΔG_T decreases linearly with denaturant concentration, [D], as[81−84]

$$\Delta G_T = \Delta G_T^\circ - m[D] \quad (6)$$

dx.doi.org/10.1021/bi500356c | *Biochemistry* 2014, 53, 5221−5235

where ΔG_T° is the Gibbs free energy of denaturation in the absence of denaturant and m is an empirical parameter (m value) that reflects the difference between the accessibility of surface areas of native and denatured states of the polypeptide chain for a given denaturant.[85−88] The inset of Figure 7a shows plots of ΔG_T versus GdnHCl concentration for ferrocyt c in the absence and presence of 1.0 M GB at pH 7.0. Insets of panels b and c of Figure 7 shows plots of ΔG_T versus GdnHCl concentration for ferricyt c at pH 7.0 and 3.8, respectively, in the absence and presence of 1.0 M GB at pH 7.0. In the absence and presence of 1.0 M GB, ΔG_T decreases linearly with GdnHCl concentration (insets of Figure 7a−c). However, in the presence of 1.0 M GB, ΔG_T decreases to a lesser extent at pH 7.0 (insets of Figure 7a,b) and decreases to a greater extent at pH 3.8 (inset of Figure 7c). These findings indicate that GB counteracts the destabilizing action of the denaturant on the thermal stability of the protein at neutral pH and exhibits a cumulative effect on the destabilizing action of the denaturant on the thermal stability of the protein at mildly acidic pH values. The m value of ferricyt c for GdnHCl in the absence and presence of GB is also estimated at pH 7.0 and 3.8 from linear least-squares fitting of the data (ΔG_T vs [D]) to eq 6 (insets of Figure 7b,c and Table S5 of the Supporting Information). Data in Table S5 clearly show that at pH 7.0 and 3.8, the presence of GB in the reaction medium changes the m value of ferricyt c for GdnHCl. It is most likely that the interactions between GB and the denaturant affect the slope of this plot. The pioneering work by Record and co-workers has described that the interactions of the solute ($GdnH^+$, urea, or GB) with certain groups of protein (amide O, aliphatic C, and aromatic C) provide the main contributions to the m value.[89] $GdnH^+$ has multiple hydrogen bond donors, but GB does not have any hydrogen bond donor.[89] The current docking results suggest that $GdnH^+$ forms a hydrogen bond with the C═O group of peptide bonds but GB does not form such hydrogen bonds (Table S2 of the Supporting Information). GB also forms a hydrogen bond with the N−H group of peptide bonds, but $GdnH^+$ acts exclusively as a hydrogen bond donor and does not form a hydrogen bond with the N−H group of peptide bonds (Table S2 of the Supporting Information). GB does not interact preferentially with the N−H group of the peptide bond because only one GB molecule is engaged with the N−H group of the peptide bond (Table S2 of the Supporting Information). However, GB interacts more preferentially with the cationic nitrogen of Arg and Lys by forming a hydrogen bond as compared to the N−H group of the peptide bond. $GdnH^+$ but not GB interacts preferentially with the carboxylate/side chain oxygen of Glu, Asp, and Asn residues by forming hydrogen bonds. These interactions between the denaturant and different groups of the protein are destabilizing, while the interactions of GB with different groups of the protein are stabilizing.[89]

At pH 7.0, as the $GdnH^+$ concentration is increased in the mixture of $GdnH^+$ and GB, the extent of the GB−$GdnH^+$ interaction also increases, which as a result weakens the denaturing power of $GdnH^+$ than in the absence of GB. Because of these concentration-dependent GB−$GdnH^+$ interactions, ΔG_T values do not show similar additive behavior over the entire GdnHCl concentration range, which as a result affects the slope of the plot of ΔG_T vs denaturant concentration. An earlier report has shown that the protonated GB at mildly acidic pH values can interact preferentially with the protein backbone and thus can act as a denaturant.[42] At pH 3.8, as the $GdnH^+$ concentration is increased in the mixture of $GdnH^+$ and GB, both solutes compete with each other for making destabilizing interactions with some common sites of the protein, which as a result affects the slope of the plot of ΔG_T versus denaturant concentration.

Effect of GB on the ΔG_D and C_m Values of Cyt c in an Aqueous Solution. Panels a and b of Figure 8 show the

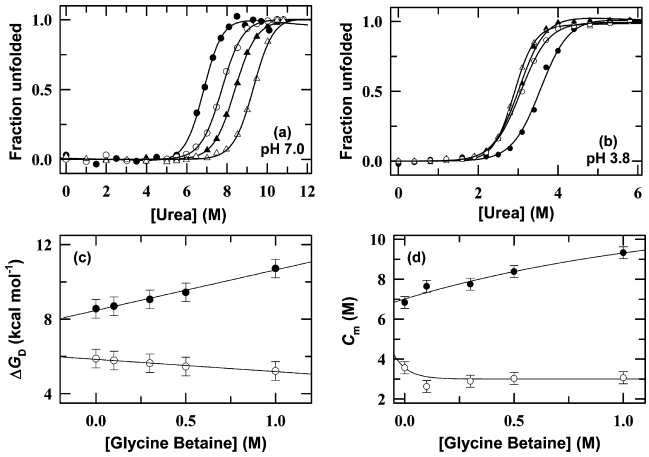

Figure 8. (a and b) Fluorescence-monitored normalized equilibrium urea-induced unfolding curves of ferricyt c at pH 7.0 and 3.8, respectively, in the presence of 0.0 (●), 0.3 (○), 0.5 (▲), and 1.0 M GB (△) at 25 °C. The solid curves represent nonlinear least-squares fits according to the standard two-state equation.[78] (c) Variation of the change in unfolding free energy, ΔG_D, of ferricyt c with GB concentration at pH 7.0 (●) and 3.8 (○). (d) Variation of the urea unfolding midpoint, C_m, of ferricyt c with GB concentration at pH 7.0 (●) and 3.8 (○).

fluorescence-monitored normalized urea-induced unfolded curves of ferricyt c at pH 7.0 and 3.8, respectively, in the absence and presence of ∼0.3, 0.5, and 1.0 M GB at 25 °C. The urea-induced unfolded curve of ferricyt c shifts toward the higher concentration of urea in the presence of GB at pH 7.0 and shifts toward the lower concentration of urea at pH 3.8. Two-state analysis[78] of the urea-induced unfolded curves of ferricyt c [Figure 8a (pH 7.0) and Figure 8b (pH 3.8)] provided the ΔG_D and m_g values at different GB concentrations (Table 3). The urea unfolding midpoint, C_m ($=\Delta G_D/m_g$), for different GB concentrations was also calculated (Table 3). As the GB concentration is increased from 0.0 to 1.0 M, ΔG_D and C_m increase at pH 7.0 and decrease at pH 3.8 (Figure 8c,d). The increase in ΔG_D in the presence of GB at pH 7.0 indicates that GB increases the thermodynamic stability of the native protein at neutral pH. On the other hand, the decrease in ΔG_D in the presence of GB at pH 3.8 suggests that GB decreases the thermodynamic stability of the native protein at mildly acidic pH values.

Effect of GB on the Denaturant-Dependent ΔG_D and C_m Values of Cyt c. Panels a and b of Figure 9 show that at pH 7.0 and 3.8, the inclusion of GdnHCl shifts the urea-induced unfolding curve to lower urea concentrations. However, in the presence of 0.5 M GB, the GdnHCl-triggered shift in the urea-induced unfolding curve is less pronounced at pH 7.0 (Figure 9a) and more pronounced at pH 3.8 (Figure 9b). To determine the effect of GB on the GdnHCl dependence of ΔG_D and m_g, the urea-induced unfolded curves of ferricyt c collected at various GdnHCl concentration in the absence and presence of 0.5 M GB were analyzed by using a

dx.doi.org/10.1021/bi500356c | Biochemistry 2014, 53, 5221−5235

Table 3. Dependence of the ΔG_D, m_g, and C_m Values of Ferricyt *c* on GB Concentration at pH 7.0 and 3.8 As Monitored by Trp Fluorescence (excitation at 280 and emission at 365 nm)[a]

	pH 7.0				pH 3.8		
[GB] (M)	C_m (M)	ΔG_D (kcal mol^{-1})	m_g (kcal mol^{-1} M^{-1})	[GB] (M)	C_m (M)	ΔG_D (kcal mol^{-1})	m_g (kcal mol^{-1} M^{-1})
0.0	6.8	8.6	1.25	0.0	3.6	5.9	1.7
0.1	7.6	8.7	1.14	0.1	2.6	5.8	2.2
0.3	7.8	9.1	1.13	0.3	2.9	5.6	2.0
0.5	8.4	9.4	1.13	0.5	3.0	5.5	1.8
1.0	9.3	10.7	1.14	1.0	3.1	5.2	1.7

[a]The uncertainties associated with ΔG_D, m_g, and C_m are ±0.5 kcal mol^{-1}, ±0.2 kcal mol^{-1} M^{-1}, and ±0.2 M, respectively.

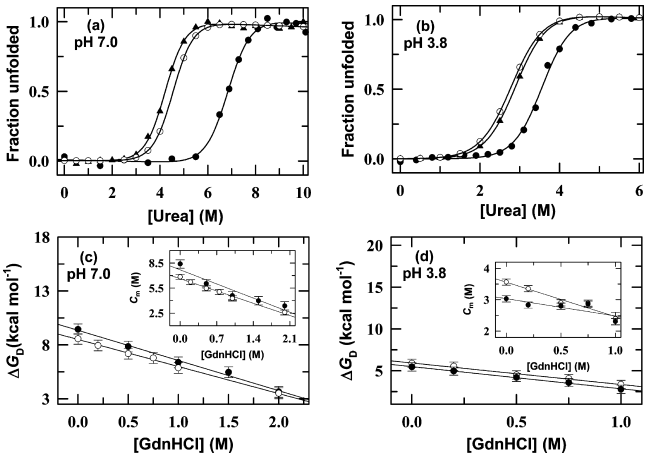

Figure 9. (a) Urea-induced denaturation curves of ferricyt *c* at pH 7.0 and 25 °C, in the absence of an additive (●), in the presence of 1.0 M GdnHCl (▲), and in the presence of 1.0 M GdnHCl with 0.5 M GB (○). (b) Urea-induced denaturation curves of ferricyt *c* at pH 3.8 and 25 °C, in the absence of an additive (●), in the presence of 0.5 M GdnHCl (▲), and in the presence of 0.5 M GdnHCl with 0.5 M GB (○). The solid curves in panels a and b represent nonlinear least-squares fits of the data according to the standard two-state equation.[78] (c and d) Variation of the change in unfolding free energy, ΔG_D, of ferricyt *c* with GdnHCl concentration in the absence (○) and presence (●) of 0.5 M GB at pH 7.0 and 3.8, respectively. The insets of panels c and d show the variation of the urea unfolding midpoint, C_m, of ferricyt *c* in the absence (○) and presence (●) of 0.5 M GB at pH 7.0 and 3.8, respectively.

two-state equation.[78] The resulting ΔG_D and m_g values are listed in Table S6 of the Supporting Information. The urea unfolding midpoint, C_m (=$\Delta G_D/m_g$), for different GdnHCl concentrations was also calculated in the absence and presence of GB (Table S6 of the Supporting Information). The data in Table S6 of the Supporting Information clearly show that at pH 7.0 and 3.8, the m_g value calculated in the absence and presence of GB is not greatly changed. At pH 7.0 and 3.8, ΔG_D and C_m decrease linearly with GdnHCl concentration (Figure 9c,d and insets of Figure 9c,d). However, in the presence of 0.5 M GB, the decrease in ΔG_D and C_m with GdnHCl concentration is less pronounced at pH 7.0 (Figure 9c and inset of Figure 9c) and more pronounced at pH 3.8 (Figure 9d and inset of Figure 9d). These findings indicate that the GB counteracts the denaturing action of GdnHCl at neutral pH while it shows an additive effect on the denaturing action of GdnHCl at mildly acidic pH values.

DISCUSSION

Kinetic and thermodynamic studies of NCO in the presence of different concentrations of GB or a denaturant (GdnHCl or urea) have provided evidence of the internal motional constraints and entropy reduction of NCO in the presence of GB and subdenaturing concentrations of the denaturant. The probable explanations for the restricted dynamics of the protein in the presence of GB and subdenaturing concentrations of urea and GdnHCl as well as the effect of GB on structural fluctuations of the protein across the folding−unfolding transition are discussed. Thermal and chemical denaturation studies of native ferrocyt *c* at pH 7.0 and ferricyt *c* at pH 7.0 and 3.8 in the presence of different concentrations of GB have provided evidence that GB increases the thermodynamic stability of the native protein at neutral pH but decreases it at mildly acidic pH values. The probable explanations for why GB increases the thermodynamic stability of the native protein at neutral pH but decreases it at mildly acidic pH values as well as the effect of GB on the GdnHCl-dependent thermodynamic stability of the native protein at pH 7.0 and 3.8 are discussed.

How Could GB, Urea, and GdnHCl Restrict the Internal Dynamics of Ferrocyt *c*? Figure 1c shows that as the GB concentration is increased, log k_{diss} decreases monoexponentially. Figure 2b shows that as the denaturant concentration is increased from 0.0 to 5.0 M GdnHCl or 9.5 M urea, log k_{diss} initially decreases and then increases, showing a minimum at ∼2.5 M GdnHCl or ∼5.5 M urea. These results provide primary evidence that GB and subdenaturing concentrations of the denaturant restrict the internal dynamics of NCO. If the internal dynamics of the protein is restricted in the presence of GB or subdenaturing concentrations of the denaturant, then the restricted dynamics should decrease the amplitude of structural fluctuation of the protein. Some earlier hydrogen exchange (HX) experiments have also shown that osmolytes such as sugar decrease the amplitude of structural fluctuation of native proteins.[37,76,90−94] Because both entropy and fluctuation have the same origin, therefore, the restricted dynamics in the presence of GB or a subdenaturing amount of denaturant must alter the conformational entropy of the protein. The data in Table 1 clearly show in the absence of additives the increase in the conformational entropy loss in the presence of 1.0 M GB, 2.5 M GdnHCl, and 5.5 M urea. These results suggest that GB and subdenaturing concentrations of urea or GdnHCl decrease the degree of motional freedom of NCO and thus restrict the internal dynamics of the native protein. Few recent reports have shown that urea forms hydrogen bonds to both C═O and N−H groups of the peptide bond while $GdnH^+$ forms hydrogen bonds to only the C═O group of the peptide bond.[95,96] A very recent report reveals that GB also forms hydrogen bonds with the N−H group of the peptide bond.[89] These findings suggest that in an aqueous solution, urea can act as a good hydrogen bond donor and acceptor while $GdnH^+$ and GB can act as a hydrogen bond donor and acceptor, respectively.[89,95,96] Results of docking between ferrocyt *c* and GB or the denaturant (urea

dx.doi.org/10.1021/bi500356c | *Biochemistry* 2014, 53, 5221−5235

or $GdnH^+$) reveal that the denaturant forms polyfunctional interactions with different groups of the protein (Figure 3a,b and Table S1 of the Supporting Information) while GB forms only a direct single hydrogen bond with the protein group (Figure 3c and Table S1 of the Supporting Information). Few earlier reports have shown that the denaturant-mediated polyfunctional interactions with different groups of cyt *c* restrict the internal dynamics of the protein.[55,77] However, osmolytes such as GB do not involve any kind of polyfunctional interactions with different groups of the protein (Figure 3c and Table S1 of the Supporting Information) and still restrict the internal dynamics of the protein (Figure 1c). How could GB restrict the internal dynamics of the protein without making any polyfunctional interaction? Figure 3c shows that GB forms a direct single hydrogen bond with different side chains of Lys or Arg residues of ferrocyt *c* or the N−H group of the peptide bond (Table S1 of the Supporting Information). Figure 3d shows that in addition to direct hydrogen bonding, GB also interacts with the protein surface via indirect polar and hydrophobic interactions (Table S2 of the Supporting Information). We can speculate that GB-mediated restricted dynamics of ferrocyt *c* originates from both direct interactions of GB with different side chains of Lys or Arg residues of the protein or the N−H group of the peptide bond and indirect interaction of GB with the protein surface.

Effects of GB on the Structural Fluctuation of NCO across the Folding−Unfolding Transition of the Protein. Pioneering works by Englander and co-workers have shown that the subglobal unfolding units of cyt *c* govern a limited set of folding pathways.[54,75,79,97−100] Therefore, it is important to evaluate the effect of GB on the thermal motions of NCO across the folding−unfolding transition. As the denaturant concentration is increased from 0.0 to 5.0 M GdnHCl or 9.5 M urea, log k_{diss} first decreases up to ∼2.5 M GdnHCl or ∼5.5 M urea and then increases (Figure 2b). The linear decrease in log k_{diss} with denaturant concentration indicates that the amplitudes of structural fluctuation of the NCO state progressively decrease within the subdenaturing limit of the denaturant. We have recently shown that within the subdenaturing limit of the denaturant, the polyfunctional interactions between protein groups and the denaturant decrease the conformational entropy and thus restrict the internal dynamics of the protein.[57,77] Because both GB and subdenaturing concentrations of the denaturant individually decrease the amplitudes of structural fluctuation of the protein (Figures 1c and 2b), the coexistence of two in reaction medium is expected to produce a cumulative effect on the constrained dynamics of NCO. In the subdenaturing limit of the denaturant, the increase in the conformational entropy loss for the CO dissociation reaction is more pronounced in the presence of GB than in its absence (Figure 2d,e and Table 1). This finding indicates that the excluded volume interactions of GB also contribute to the constrained dynamics of NCO.[36] En route from subdenaturing to denaturing conditions, large-scale unfolding fluctuation dominates the dynamics,[55] which increases the configurational entropy and decreases the activation enthalpy and activation entropy (Table 1). Remarkably, the extents of the decreases in activation enthalpy and activation entropy are smaller in the presence of GB than in its absence (Table 1), indicating that GB opposes the structural fluctuations that result in unfolding of the protein.

Results of docking between ferrocyt *c* and GB or the denaturant (urea or $GdnH^+$) reveal that the denaturant forms polyfunctional interactions with different groups of the protein (Figure 3a,b and Table S1 of the Supporting Information) while GB forms only a direct single hydrogen bond with the protein group (Figure 3c and Table S1 of the Supporting Information). In addition, GB also forms a contact with the protein surface via indirect polar and hydrophobic interactions (Table S2 of the Supporting Information). We can speculate that within the subdenturing limit of the denaturant, the polyfunctional interactions of the denaturant with different groups of the protein and the direct interactions of GB with different side chains of Lys or Arg residues of the protein or the N−H group of the peptide bond as well as the indirect interaction of GB with the protein surface restrict the internal dynamics of the protein. En route from subdenaturing to denaturing conditions, the large-scale subglobal unfolding motions dominate the dynamics, and under strongly destabilizing conditions, global unfolding completely takes over.[57,77] Thus, it is possible that in the subdenaturing to denaturing milieu, the direct interactions of GB with different side chains of Lys or Arg residues of the protein or the N−H group of the peptide bond as well as the indirect interactions of GB with the protein surface oppose the structural fluctuations that cause unfolding of the protein.

How Does GB Modulate the Thermodynamic Stability of Native Cyt *c* at Neutral and Mildly Acidic pH Values? The results presented here show that at neutral pH, GB increases the thermodynamic stability of native ferrocyt *c* (Figures 2a and 5a,b) and ferricyt *c* (Figures 5c and 8c). This result is consistent with an earlier report that found that GB increases the thermal stability of α-lactalbumin, RNase A, and lysozyme at neutral pH.[42] A recent report by Singh et al. shows that the effect of GB at acidic pH values may vary from one protein to another.[42] They showed that at acidic pH values, GB decreases the thermal stability of α-lactalbumin, increases the thermal stability of RNase A, and does not change the thermal stability of lysozyme significantly. Our results show that GB decreases the thermodynamic stability of ferricyt *c* at pH 3.8 (Figures 5d and 8c). How could GB increase the thermodynamic stability of native ferricyt *c* at neutral pH but decrease it at mildly acidic pH values? In general, the preferential exclusion of the osmolyte stabilizes the proteins while preferential binding of the osmolyte destabilizes the proteins.[101] It may be possible that at neutral pH, zwitterionic GB is excluded from the protein surface because of unfavorable interaction with the protein backbone, i.e., act as stabilizers, while in its positively charged form at low pH, it directly interacts with the protein backbone, preferentially stabilizing the denatured state and decreasing the free energy of unfolding, ΔG_{D-N}.[42,102,103]

GB Counteracts the Destabilizing Actions of the Denaturant at Neutral pH and Shows an Additive Effect with the Denaturant at Acidic pH Values. The denaturing actions of urea and $GdnH^+$ are generally based on their ability to bind with the protein.[55,104−106] Within the pH range from 7.0 to 3.8, the thermodynamic stabilities of native ferrocyt *c* (Figure 6d) and native ferricyt *c* (Figures 6e,f and 9c,d) decrease in the presence of the denaturant. However, the inclusion of GB results in the counteraction of the destabilizing action of the denaturant at neutral pH 7.0 (Figures 6d,e and 9c) and has an additive effect on the denaturing action of the denaturant at pH 3.8 (Figures 6f and 9d). Timasheff et al. have reported that the TMAO counteracts the denaturing effect of urea mainly by shifting the equilibrium between preferential binding of urea and preferential exclusion of TMAO, which

dx.doi.org/10.1021/bi500356c | *Biochemistry* 2014, 53, 5221−5235

results in the enhanced hydration of the protein.[13,107] Similarly, in case of cyt *c* at pH 7.0, it is possible that the addition of GB alters the balance between the preferential binding of the denaturant and preferential exclusion of GB, resulting in an increased level of hydration of the protein, and helps in the counteraction of the destabilizing action of the denaturant. However, at pH 3.8, it is possible that the preferential binding interactions of both the denaturant and protonated GB show a cumulative effect on the destabilization of the protein.

Mechanism of Osmolyte-Induced Protein Stabilization. Timasheff and co-workers have shown that the major driving force for osmolyte-induced stabilization of proteins is the preferential exclusion of the osmolyte from the immediate vicinity of the protein domain.[108,109] The pioneering work by Bolen has shown that the terms preferential exclusion of osmolyte and preferential hydration of protein are interchangeable and indicate the same phenomenon.[110] Accordingly, these results indicate that the GB stabilizes the ferricyt *c* at pH 7.0 because it exists in zwitterionic form and is excluded from the protein surface. However, in its positively charged form at low pH values, it directly interacts with the protein backbone and hence destabilizes the protein.[42,102,103]

By using the transfer model, Timasheff and co-workers and Bolen demonstrated that the osmolytes stabilize the proteins mainly by interacting with the denatured state, leaving the native state comparatively unaltered and functional.[13,110] A recent theoretical study involving the molecular dynamics simulations of a number of model peptides in an aqueous solution of TMAO has shown that the entropic stabilization of proteins in a crowded environment is due to excluded volume interactions.[36] Bolen et al. have reported that the unfavorable interaction between the backbone and protecting osmolytes increases the stability of proteins by increasing the chemical potential of the denatured state and by producing a collateral effect that contracts the denatured state.[111] The contraction decreases the conformational entropy of the denatured state and increases the density of the hydrophobic groups.[111] These two effects also contribute to the ability of protecting osmolytes to force proteins to fold.[111] Recently, Thirumalai et al. studied the effects of TMAO on the stability of RNA hairpins and revealed that TMAO preferentially interacts with the base through the formation of a single hydrogen bond.[112] The current docking results also reveal that some GB molecules form a single hydrogen bond with different side chains of Lys or Arg residues of the protein, while others are also in contact with the protein surface via indirect interactions (polar or hydrophobic) and hence stabilize the protein at pH 7.0.

■ ASSOCIATED CONTENT

Supporting Information

Figures S1 and S2 and Tables S1−S6. This material is available free of charge via the Internet at http://pubs.acs.org.

■ AUTHOR INFORMATION

Corresponding Author

*E-mail: rajesh.kumar@thapar.edu. Phone: 91-175-239-3832. Fax: 91-175-236-4498.

Funding

This work was supported by a Council of Scientific and Industrial Research grant [to R.K., 37(148s)/1r/EMR-II], a UGC Major research grant [to R.K., 41-258/2012 (SR)], a Department of Science and Technology SERC Fast Track Research Grant (to R.K., Project SR/FT/CS-070/2009), a Ramalingaswami Re-entry Fellowship from the Department of Biotechnology (DBT), India (to D.S., BT/RLF/RE-ENTRY-33-2010), a DST/INSPIRE Fellowship (to R.J., Fellowship IF 110240), and the Government of India.

Notes

The authors declare no competing financial interest.

■ ACKNOWLEDGMENTS

We greatly acknowledge the many helpful and kind suggestions of Dr. Abani K. Bhuyan and Dr. Aurdien Grosdidier.

■ ABBREVIATIONS

GB, glycine betaine; GdnHCl, guanidine hydrochloride; ferrocyt *c*, ferrocytochrome *c*; CD, circular dichroism; NCO, natively folded carbonmonoxycytochrome *c*; Lys, lysine; Arg, arginine.

■ REFERENCES

(1) Kuzmenkina, E. V., Heyes, C. D., and Nienhaus, G. U. (2005) Single-molecule Forster resonance energy transfer study of protein dynamics under denaturing conditions. *Proc. Natl. Acad. Sci. U.S.A. 102*, 15471−15476.

(2) Yancey, P. H., and Somero, G. N. (1979) Counteraction of urea destabilization of protein structure by methylamine osmoregulatory compounds of elasmobranch fishes. *Biochem. J. 183*, 317−323.

(3) Yancey, P. H., Clark, M. E., Hand, S. C., Bowlus, R. D., and Somero, G. N. (1982) Living with water stress: Evolution of osmolyte systems. *Science 217*, 1214−1222.

(4) Yancey, P. H., Blake, W. R., and Conley, J. (2002) Unusual organic osmolytes in deep-sea animals: Adaptations to hydrostatic pressure and other perturbants. *Comp. Biochem. Physiol. 131B*, 667−676.

(5) Venkatesu, P., Lee, M. J., and Lin, H. M. (2007) Trimethylamine N-oxide counteracts the denaturing effects of urea or GdnHCl on protein denatured state. *Arch. Biochem. Biophys. 466*, 106−115.

(6) Strambini, G. B., and Gonnelli, M. (2008) Singular efficacy of trimethylamine N-oxide to counter protein destabilization in ice. *Biochemistry 47*, 3322−3331.

(7) Venkatesu, P., Lee, M. J., and Lin, H. M. (2009) Osmolyte counteracts urea-induced denaturation of α-chymotrypsin. *J. Phys. Chem. B 113*, 5327−5338.

(8) Timasheff, S. N. (2002) Protein−solvent preferential interactions, protein hydration and the modulation of biochemical reactions by solvent components. *Proc. Natl. Acad. Sci. U.S.A. 99*, 9721−9726.

(9) Bolen, D. W., and Baskakov, I. V. (2001) The osmophobic effect: Natural selection of a thermodynamic force in protein folding. *J. Mol. Biol. 310*, 955−963.

(10) Niebuhr, M., and Koch, M. H. J. (2005) Effects of urea and trimethylamine-N-oxide (TMAO) on the interactions of lysozyme in solution. *Biophys. J. 89*, 1978−1983.

(11) Bennion, B. J., and Daggett, V. (2003) The molecular basis for the chemical denaturation of proteins by urea. *Proc. Natl. Acad. Sci. U.S.A. 100*, 5142−5147.

(12) Yancey, P. H., and Siebenaller, J. F. (1999) Trimethylamine oxide stabilizes teleost and mammalian lactate dehydrogenases against inactivation by hydrostatic pressure and trypsinolysis. *J. Exp. Biol. 202*, 3597−3603.

(13) Lin, T. Y., and Timasheff, S. N. (1994) Why do some organisms use a urea-methylamine mixture as osmolyte? Thermodynamic compensation of urea and trimethylamine N-oxide interactions with protein. *Biochemistry 33*, 12695−12701.

(14) Baskakov, I. V., and Bolen, D. W. (1998) Time-dependent effects of trimethylamine-N-oxide/urea on lactate dehydrogenase activity: An unexplored dimension of the adaptation paradigm. *Biophys. J. 74*, 2658−2665.

(15) Baskakov, I. V., Wang, A. J., and Bolen, D. W. (1998) Trimethylamine-N-oxide counteracts urea effects on rabbit muscle lactate dehydrogenase function: A test of the counteraction hypothesis. *Biophys. J. 74*, 2666−2673.
(16) Wang, A. J., and Bolen, D. W. (1997) A naturally occurring protective system in urea-rich cells: Mechanism of osmolyte protection of proteins against urea denaturation. *Biochemistry 36*, 9101−9108.
(17) Tseng, H. C., and Graves, D. J. (1998) Natural methylamine osmolytes, trimethylamine N-oxide and betaine, increase tau-induced polymerization of microtubules. *Biochem. Biophys. Res. Commun. 250*, 726−730.
(18) Tatzelt, J., Prusiner, S. B., and Welch, W. J. (1996) Chemical chaperones interfere with the formation of scrapie prion protein. *EMBO J. 15*, 6363−6373.
(19) Xie, G. F., and Timasheff, S. N. (1997) Temperature dependence of the preferential interactions of ribonuclease A in aqueous co-solvent systems: Thermodynamic analysis. *Protein Sci. 6*, 222−232.
(20) Xie, G. F., and Timasheff, S. N. (1997) Mechanism of the stabilization of ribonuclease A by sorbitol: Preferential hydration is greater for the denatured then for the native protein. *Protein Sci. 6*, 211−221.
(21) Xie, G. F., and Timasheff, S. N. (1997) The thermodynamic mechanism of protein stabilization by trehalose. *Biophys. Chem. 64*, 25−43.
(22) Lin, T. Y., and Timasheff, S. N. (1996) On the role of surface tension in the stabilization of globular proteins. *Protein Sci. 5*, 372−381.
(23) Zou, Q., Bennion, B. J., Daggett, V., and Murphy, K. (2002) The molecular mechanism of stabilization of proteins by TMAO and its ability to counteract the effects of urea. *J. Am. Chem. Soc. 124*, 1192−1202.
(24) Wang, A. J., and Bolen, D. W. (1996) Effect of proline on lactate dehydrogenase activity: Testing the generality and scope of the compatibility paradigm. *Biophys. J. 71*, 2117−2122.
(25) Street, T. O., Bolen, D. W., and Rose, G. D. (2006) A molecular mechanism for osmolyte-induced protein stability. *Proc. Natl. Acad. Sci. U.S.A. 103*, 13997−14002.
(26) Bolen, D. W. (2004) Effects of naturally occurring osmolytes on protein stability and solubility: Issues important in protein crystallization. *Methods 34*, 312−322.
(27) Attri, P., Venkatesu, P., and Lee, M. J. (2010) Influence of osmolytes and denaturants on the structure and enzyme activity α-chymotrypsin. *J. Phys. Chem. B 114*, 1471−1478.
(28) Venkatesu, P., Lee, M. J., and Lin, H. M. (2008) Effect of osmolyte or GdnHCl on volumetric properties of aqueous solutions containing cyclic dipeptides. *Biochem. Eng. J. 38*, 326−340.
(29) Ortiz-Costa, S., Sorenson, M. M., and Sola-Penna, M. (2008) Betaine protects urea-induced denaturation of myosin subfragment-1. *FEBS J. 275*, 3388−3396.
(30) Venkatesu, P., Lee, M. J., and Lin, H. M. (2007) Thermodynamic characterization of the osmolyte effect on protein stability and the effect of GdnHCl on the protein denatured state. *J. Phys. Chem. B 111*, 9045−9056.
(31) Frauenfelder, H., McMahon, B. H., Austin, R. H., Chu, K., and Groves, J. T. (2001) The role of structure, energy landscape, dynamics, and allostery in the enzymatic function of myoglobin. *Proc. Natl. Acad. Sci. U.S.A. 98*, 2370−2374.
(32) Fenimore, P. W., Frauenfelder, H., McMahon, B. H., and Parak, F. G. (2002) Slaving: Solvent fluctuations dominate protein dynamics and functions. *Proc. Natl. Acad. Sci. U.S.A. 99*, 16047−16051.
(33) Fenimore, P. W., Frauenfelder, H., McMahon, B. H., and Young, R. D. (2004) Bulk-solvent and hydration-shell fluctuations, similar to α and β-fluctuations in glass, control protein motions and fluctuations. *Proc. Natl. Acad. Sci. U.S.A. 101*, 14408−14413.
(34) Ansari, A., Jones, C. M., Henry, E. R., Hofrichter, J., and Eaton, W. A. (1992) The role of solvent viscosity in the dynamics of protein conformational change. *Science 256*, 1796−1798.
(35) Beece, D., Eisenstein, L., Frauenfelder, H., Good, D., Marden, M. C., Reinisch, L., Reynolds, A. H., Sorensen, L. B., and Yue, K. T. (1980) Solvent viscosity and protein dynamics. *Biochemistry 19*, 5147−5157.
(36) Cho, S. S., Reddy, G., Straub, J. E., and Thirumalai, D. (2011) Entropic stabilization of proteins by TMAO. *J. Phys. Chem. B 115*, 13401−13407.
(37) Wang, A., Robertson, A. D., and Bolen, D. W. (1995) Effects of naturally occurring compatible osmolyte on the internal dynamics of ribonuclease A. *Biochemistry 34*, 15096−15104.
(38) Zhadin, N., and Callender, R. (2011) Effect of osmolytes on protein dynamics in the lactate dehydrogenase-catalyzed reaction. *Biochemistry 50*, 1582−1589.
(39) Santoro, M. M., Liu, Y., Khan, S. M. A., Hou, L. X., and Bolen, D. W. (1992) Increased thermal stability of proteins in the presence of naturally occurring osmolytes. *Biochemistry 31*, 5278−5283.
(40) Singh, R. K., Haque, I., and Ahmad, F. (2005) Counteracting Osmolyte Trimethylamine *N*-Oxide Destabilizes Proteins at pH below its p*Ka*. *J. Biol. Chem. 280*, 11035−11042.
(41) Singh, L. R., Poddar, N. K., Dar, T. A., Kumar, R., and Ahmad, F. (2011) Protein and DNA desatabilization by osmolytes: The other side of the coin. *Life Sci. 88*, 117−125.
(42) Singh, L. R., Dar, T. A., Rahman, S., Jamal, S., and Ahmad, F. (2009) Glycine betaine may have opposite effects on protein stability at high and low pH values. *Biochim. Biophys. Acta 1794*, 929−935.
(43) Schellman, J. A. (2002) Fifty years of solvent denaturation. *Biophys. Chem. 96*, 91−101.
(44) Bhuyan, A. K., and Kumar, R. (2002) Kinetic barriers to the folding of horse cytochrome *c* in the reduced state. *Biochemistry 41*, 12821−12834.
(45) Bhuyan, A. K., and Udgaonkar, J. B. (2001) Folding of horse cytochrome *c* in the reduced state. *J. Mol. Biol. 312*, 1135−1160.
(46) Prabhu, N. P., Kumar, R., and Bhuyan, A. K. (2004) Folding barrier in horse cytochrome *c*: Support for a classical folding pathway. *J. Mol. Biol. 337*, 195−208.
(47) Kumar, R., and Bhuyan, A. K. (2005) Two-state folding of horse ferrocytochrome *c*: Analyses of linear free energy relationship, chevron curvature, and stopped-flow burst relaxation kinetics. *Biochemistry 44*, 3024−3033.
(48) Bhuyan, A. K., Rao, D. K., and Prabhu, N. P. (2005) Protein folding in classical perspective: Folding of horse cytochrome *c*. *Biochemistry 44*, 3034−3040.
(49) Courtenay, E. S., Capp, M. W., Anderson, C. F., and Record, M. T., Jr. (2000) Vapor pressure osmometry studies of osmolyte−protein interactions: Implications for the action of osmoprotectants in vivo and for the interpretation of "osmotic stress" experiments in vitro. *Biochemistry 39*, 4455−4471.
(50) Record, M. T., Jr., Zhang, W., and Anderson, C. F. (1998) Analysis of effects of salts and uncharged solutes on protein and nucleic acid equilibria and processes: A practical guide to recognizing and interpreting polyelectrolyte effects, Hofmeister effects, and osmotic effects of salts. *Adv. Protein Chem. 51*, 281−353.
(51) Felitsky, D. J., Cannon, J. G., Capp, M. W., Hong, J., Wynsberghe, A. W. V., Anderson, C. F., and Record, M. T., Jr. (2004) The exclusion of glycine betaine from anionic biopolymer surface: Why glycine betaine is an effective osmoprotectant but also a compatible solute. *Biochemistry 43*, 14732−14743.
(52) Frauenfelder, H., Parak, F., and Young, R. D. (1988) Conformational substates in proteins. *Annu. Rev. Biophys. Biophys. Chem. 17*, 451−479.
(53) Schlichting, I., Berendzen, J., Phillips, G. N., and Sweet, R. M. (1994) Crystal structure of photolysed carbonmonoxy-myoglobin. *Nature 371*, 808−812.
(54) Bai, Y., Sosnick, T. R., Mayne, L., and Englander, S. W. (1995) Protein folding intermediates: Native-state hydrogen exchange. *Science 269*, 192−197.
(55) Bhuyan, A. K. (2002) Protein stabilization by urea and guanidine hydrochloride. *Biochemistry 41*, 13386−13394.

(56) Varhac, R. (2013) Urea-induced modification of cytochrome *c* flexibility as probed by cyanide binding. *Biochim. Biophys. Acta 183*, 739−744.
(57) Kumar, R., Prabhu, N. P., Yadaiah, M., and Bhuyan, A. K. (2004) Protein stiffening and entropic stabilization in the subdenaturing limit of guanidine hydrochloride. *Biophys. J. 87*, 2656−2662.
(58) Pace, C. N., Shirley, B. A., and Thomson, J. A. (1989) in *Measuring the conformational stability of a protein in Protein Structure: A Practical Approach* (Creighton, T. E., Ed.) pp 311−330, IRL Press, Oxford, U.K.
(59) Qi, P. X., Beckman, R. A., and Wand, A. J. (1996) Solution structure of horse heart ferricytochrome *c* and detection of redox-related structural changes by high-resolution ^{1}H NMR. *Biochemistry 35*, 12275−12286.
(60) Grosdidier, A., Zoete, V., and Michielin, O. (2011) SwissDock, a protein-small molecule docking web service based on EADock DSS. *Nucleic Acids Res. 39*, W270−W277.
(61) Grosdidier, A., Zoete, V., and Michielin, O. (2011) Fast docking using the CHARMM force field with EADock DSS. *J. Comput. Chem. 32*, 2149−2159.
(62) Guha, R., Howard, M. T., Hutchison, G. R., Murray-Rust, P., Rzepa, H., Steinbeck, C., Wegner, J., and Willighagen, E. L. (2006) The Blue Obelisk-interoperability in chemical informatics. *J. Chem. Inf. Model. 46*, 991−998.
(63) Zoete, V. F., Cuendet, M., Grosdidier, A., and Michielin, O. (2011) SwissParam: A fast force field generation tool for small organic molecules. *J. Comput. Chem. 32*, 2359−2368.
(64) Halgren, T. A. (1996) Merck molecular force field. I. Basis, form, scope, parameterization, and performance of MMFF94. *J. Comput. Chem. 17*, 490−519.
(65) Halgren, T. A. (1996) Merck molecular force field. II. MMFF94 van der Waals and electrostatic parameters for intermolecular interactions. *J. Comput. Chem. 17*, 520−552.
(66) Halgren, T. A. (1996) Merck molecular force field. III. Molecular geometries and vibrational frequencies for MMFF94. *J. Comput. Chem. 17*, 553−586.
(67) Halgren, T. A. (1996) Merck molecular force field. IV. Conformational energies and geometries for MMFF94. *J. Comput. Chem. 17*, 587−615.
(68) Halgren, T. A. (1996) Merck molecular force field. V. Extension of MMFF94 using experimental data, additional computational data and empirical rules. *J. Comput. Chem. 17*, 616−641.
(69) Pettersen, E. F., Goddard, T. D., Huang, C. C., Couch, G. S., Greenblatt, D. M., Meng, E. C., and Ferrin, T. E. (2004) UCSF Chimera: A visualization system for exploratory research and analysis. *J. Comput. Chem. 13*, 1605−1612.
(70) Margoliash, E., and Frohwirt, N. (1959) Spectrum of horse-heart cytochrome *c*. *Biochem. J. 71*, 570−572.
(71) Varhac, R., Antalik, M., and Bano, M. (2004) Effect of temperature and guanidine hydrochloride on ferrocytochrome *c* at neutral pH. *JBIC, J. Biol. Inorg. Chem. 9*, 12−22.
(72) Hirato, N., Mizuno, K., and Goto, Y. (1998) Group additive contributions to the alcohol-induced α-helix formation of melittin: Implication for the mechanism of the alcohol effects on proteins. *J. Mol. Biol. 275*, 365−378.
(73) Leszczynski, J. F., and Rose, G. D. (1986) Loops in globular proteins: A novel category of secondary structure. *Science 234*, 849−855.
(74) Hoang, L., Maity, H., Krishna, M. M. G., Lin, Y., and Englander, S. W. (2003) Folding units govern the cytochrome *c* alkaline transition. *J. Mol. Biol. 331*, 37−43.
(75) Xu, Y., Mayne, L. C., and Englander, S. W. (1998) Evidence for an unfolding and refolding pathway in cytochrome *c*. *Nat. Struct. Biol. 5*, 774−778.
(76) Morgan, J. D., and McCammon, J. A. (1983) Molecular dynamics of ferrocytochrome *c*: Time dependence of the atomic displacements. *Biopolymers 22*, 1579−1593.
(77) Kumar, S., Sharma, D., and Kumar, R. (2014) Effect of urea and alkylureas on the stability and structural fluctuation of the M80-containing Ω-loop of horse cytochrome *c*. *Biochim. Biophys. Acta 1844*, 641−655.
(78) Santoro, M. M., and Bolen, D. W. (1988) Unfolding free energy changes determined by the linear extrapolation method. 1. Unfolding of phenylmethanesulfonyl α-chymotrypsin using different denaturants. *Biochemistry 27*, 8063−8068.
(79) Ohgushi, M., and Wada, A. (1983) "Molten globule state": A compact form of globular proteins with mobile side-chains. *FEBS Lett. 164*, 21−24.
(80) Ptitsyn, O. B. (1987) Protein folding: Hypothesis and experiments. *J. Protein Chem. 6*, 273−293.
(81) Liu, Z., Reddy, G., and Thirumalai, D. (2012) Theory of the molecular transfer model for proteins with applications to the folding of the src-SH3 domain. *J. Phys. Chem. B 116*, 6707−6716.
(82) Greene, R. F., and Pace, C. N. (1974) Urea and guanidine hydrochloride denaturation of ribonuclease, lysozyme, α-chymotrypsin, and α-lactoglobulin. *J. Biol. Chem. 249*, 5388−5393.
(83) Tanford, C., and Aune, K. C. (1970) Thermodynamics of the denaturation of lysozyme by guanidine hydrochloride. 3. Dependence on temperature. *Biochemistry 9*, 206−211.
(84) Poklar, N., Vesnaver, G., and Lapanje, S. (1994) Denaturation behavior of α-chymotrypsinogen A in urea and alkylurea solutions: Fluorescence studies. *J. Protein Chem. 13*, 323−331.
(85) Schellman, J. A. (1987) Selective binding and solvent denaturation. *Biopolymers 26*, 549−559.
(86) Alonso, D. O., and Dill, K. A. (1991) Solvent denaturation and stabilization of globular proteins. *Biochemistry 30*, 5974−5985.
(87) Mayo, S. L., and Baldwin, R. L. (1993) Guanidinium chloride induction of partial unfolding in amide proton exchange in RNase A. *Science 262*, 873−876.
(88) Knapp, J. A., and Pace, C. N. (1974) Guanidine hydrochloride and acid denaturation of horse, cow, and *Candida krusei* cytochromes *c*. *Biochemistry 13*, 1289−1294.
(89) Guinn, E. J., Pegram, L. M., Capp, M. W., Pollock, M. N., and Record, M. T., Jr. (2011) Quantifying why urea is a protein denaturant, whereas glycine betaine is a protein stabilizer. *Proc. Natl. Acad. Sci. U.S.A. 108*, 16932−16937.
(90) Kim, Y. S., Jones, L. S., Dong, A. C., Kendrick, B. S., Chang, B. S., Manning, M. C., Randolph, T. W., and Carpenter, J. F. (2003) Effects of sucrose on conformational equilibria and fluctuations within the native-state ensemble of proteins. *Protein Sci. 12*, 1252−1261.
(91) Butler, S. L., and Falke, J. J. (1996) Effects of protein stabilizing agents on thermal backbone motions: A disulfide trapping study. *Biochemistry 35*, 10595−10600.
(92) Kendrick, B. S., Chang, B. S., Arakawa, T., Peterson, B., Randolph, T. W., Manning, M. C., and Carpenter, J. F. (1997) Preferential exclusion of sucrose from recombinant interleukin-1 receptor antagonist: Role in restricted conformational mobility and compaction of native state. *Proc. Natl. Acad. Sci. U.S.A. 94*, 11917−11922.
(93) Cioni, P., Bramanti, E., and Strambini, G. B. (2005) Effects of sucrose on the internal dynamics of azurin. *Biophys. J. 88*, 4213−4222.
(94) Petsko, G. A., and Ringe, D. (1984) Fluctuations in protein structure from X-ray diffraction. *Annu. Rev. Biophys. Bioeng. 13*, 331−371.
(95) Lim, W. K., Rösgen, J., and Englander, S. W. (2009) Urea, but not guanidinium, destabilizes proteins by forming hydrogen bonds to the peptide group. *Proc. Natl. Acad. Sci. U.S.A. 106*, 2595−2600.
(96) O'Brien, E. P., Dima, R. I., Brooks, B., and Thirumalai, D. (2007) Interactions between hydrophobic and ionic solutes in aqueous guanidinium chloride and urea solutions: Lessons for protein denaturation mechanism. *J. Am. Chem. Soc. 129*, 7346−7353.
(97) Hoang, L., Bédard, S., Krishna, M. M. G., Lin, Y., and Englander, S. W. (2002) Cytochrome *c* folding pathway: Kinetic native-state hydrogen exchange. *Proc. Natl. Acad. Sci. U.S.A. 99*, 12173−12178.
(98) Maity, H., Maity, M., Krishna, M. M., Mayne, L., and Englander, S. W. (2005) Protein folding: The stepwise assembly of foldon units. *Proc. Natl. Acad. Sci. U.S.A. 102*, 4741−4746.

(99) Maity, H., Maity, M., and Englander, S. W. (2004) How cytochrome *c* folds, and why: Submolecular foldon units and their stepwise sequential stabilization. *J. Mol. Biol. 343*, 223−233.
(100) Krishna, M. M., Maity, H., Rumbley, J. N., Lin, Y., and Englander, S. W. (2006) Order of steps in the cytochrome *c* folding pathway: Evidence for a sequential stabilization mechanism. *J. Mol. Biol. 359*, 1410−1419.
(101) Gonnelli, M., and Strambini, G. B. (1995) Phosphorescence lifetime of tryptophan in proteins. *Biochemistry 34*, 13847−13857.
(102) Granata, V., Palladino, P., Tizzano, B., Negro, A., Berisio, R., and Zagari, A. (2006) The effect of the osmolyte trimethylamine N-oxide on the stability of the prion protein at low pH. *Biopolymers 82*, 234−240.
(103) Natalello, A., Liu, J., Ami, D., Doglia, S. M., and de Marco, A. (2009) The osmolyte betaine promotes protein misfolding and disruption of protein aggregates. *Proteins: Struct., Funct., Bioinf. 75*, 509−517.
(104) Hibbard, L. S., and Tulinsky, A. (1978) Expression of functionality of α-chymotrypsin. Effects of guanidine hydrochloride and urea in the onset of denaturation. *Biochemistry 17*, 5460−5468.
(105) Pike, A. C., and Acharya, K. R. (1994) A structural basis for the interaction of urea with lysozyme. *Protein Sci. 3*, 706−710.
(106) Dunbar, J., Yennawar, H. P., Banerji, S., Luo, J., and Farber, G. K. (1997) The effect of denaturants on protein structure. *Protein Sci. 6*, 1727−1733.
(107) Timasheff, S. N. (2002) Protein hydration, thermodynamic binding, and preferential hydration. *Biochemistry 41*, 13473−13482.
(108) Prakash, V., Loucheux, C., Scheuffle, S., Gorbunoff, J., and Timasheff, S. N. (1981) Interactions of proteins with solvent components in 8 M urea. *Arch. Biochem. Biophys. 210*, 455−464.
(109) Arakawa, T., Bhat, R., and Timasheff, S. N. (1990) Preferential interactions determine protein solubility in three-component solutions: The magnesium chloride system. *Biochemistry 29*, 1914−1923.
(110) Bolen, D. W. (2001) Protein stabilization by naturally occurring osmolytes. *Methods Mol. Biol. 168*, 17−36.
(111) Qu, Y., Bolen, C. L., and Bolen, D. W. (1998) Osmolyte-driven contraction of a random coil protein. *Proc. Natl. Acad. Sci. U.S.A. 95*, 9268−9273.
(112) Pincus, D. L., Hyeon, C., and Thirumalai, D. (2008) Effects of trimethylamine N-oxide (TMAO) and crowding agents on the stability of RNA hairpins. *J. Am. Chem. Soc. 130*, 7364−7372.